Planetary and Space Science 184 (2020) 104855

Contents lists available at ScienceDirect

Planetary and Space Science

journal homepage: www.elsevier.com/locate/pss

Mid-infrared spectroscopic investigation of meteorites and perspectives for thermal infrared observations at the binary asteroid Didymos

A. Skulteti [a], A. Kereszturi [b,c,*], M. Szabo [d], Zs Kereszty [e], F. Cipriani [f]

[a] Research Centre for Astronomy and Earth Sciences, Geographical Institute, Hungary
[b] Research Centre for Astronomy and Earth Sciences, Konkoly Thege Miklos Astronomical Institute, Hungary
[c] European Astrobiology Institute, France
[d] Research Centre for Astronomy and Earth Sciences, Institute for Geological and Geochemical Research, Hungary
[e] International Meteorite Collectors Association, Hungary
[f] European Space Agency, ESTEC/TEC-EPS, Keplerlaan 1, 2200AG, Noordwijk, the Netherlands

A B S T R A C T

Near future missions to Near Earth Asteroids could provide new information exploiting the middle-infrared (2.5–25 μm) region, as at the temperature range of asteroids at Earth' solar distance the maximal energy is emitted in this region. The IR range is ideal for the analysis and separation of various silicate types. This work reviews the background knowledge and evaluates the possibilities for mineral identification using high resolution laboratory data. Examples are presented using laboratory based meteorite powder data to evaluate the possibility for identification of plagioclase, estimation on the Mg/(Mg + Fe) ratio and other characteristics. The expected peak position shift from temperature differences on a rotating asteroid might be below 0.01 μm, while the fine structure of bands requires high spectral resolution as well. However, with moderate resolution, the analysis of three main minerals is still possible, focusing at the range of 12.5–9.09 μm (800-1100 cm^{-1}) with spectral resolution of about 0.08 μm (10 cm^{-1}), to identify the expected main bands of olivine, pyroxene and feldspars.

An infrared camera at small orbital distance around the target could resolve fine powder covered areas like dust ponds or separate blocks. For this task an angular resolution below 0.05° might be required. Such observations would provide a wide range of important data both on surface composition, granular processes and space weathering on asteroid surfaces. However, further targeted laboratory analysis is necessary, especially using pure minerals of different grain size and meteorite powder mixtures.

1. Introduction

The analysis of Near Earth Asteroids is of high importance partly because these objects are easily accessible for spacecraft (Michel et al., 2014), and samples could be returned on moderate cost (Duffard et al., 2011; Fujiwara et al., 2000; Lauretta et al., 2017). The other main reason for their analysis is the preparation for asteroid deflection to avoid a possible impact (Chapman, 1994; Cheng et al., 2016; Losiak et al., 2017; Perna et al., 2013).

This paper focuses on the **mid-infrared observational possibilities** to prepare thermal infrared observations for the HERA (formerly named AIM, Michel et al., 2016, 2018) mission of ESA that targets the Didymos double asteroid, also the target of the NASA DART impacting mission (Cheng et al., 2017; Stickle et al., 2016). This work investigates the required resolution and expected band positions for a sophisticated infrared detector in the future. Below we outline the expected scientific return of a high performance mid-infrared detector as part of the scientific payload of this mission. We identify the ideal conditions of observation, including the design of the instrument and planning of observations. Such a camera could be used for simultaneously retrieving temperature, thermal inertia, mineral composition and rock shape of the Didymos surface. In addition it would aid spacecraft navigation (Foglia Manzillo et al., 2018).

High-resolution asteroid observations in the infrared are important not only for surface processes on small bodies but also for planets, as they could provide insight into the formation and geological evolution of different bodies (Blichert-Toft and Albarède, 1997; Fintor et al., 2014; Greenwood et al., 2005; Gurgurewicz et al., 2009; MacPherson et al., 1995; Maturilli et al., 2006; Munoz Caro and Martinez-Frias, 2007), and also on the asteroid-meteorite connection (Beck et al., 2010; Nesvorný et al., 2009; Przylibski e al. 2005). Further overview of our current knowledge is presented in the next section.

1.1. Overview of current knowledge

This section is separated into three parts: 1. information on the

* Corresponding author. Research Centre for Astronomy and Earth Sciences, Konkoly Thege Miklos Astronomical Institute, Hungary.
E-mail addresses: skulteti.agnes@csfk.mta.hu (A. Skulteti), kereszturi.akos@csfk.mta.hu (A. Kereszturi).

https://doi.org/10.1016/j.pss.2020.104855
Received 19 August 2019; Received in revised form 10 January 2020; Accepted 27 January 2020
Available online 30 January 2020

spectral analysis and mineral determination by the IR DRIFT method in laboratories, 2. on the spectral characteristics of meteorite powders, and 3. on the related spectral properties of analysed asteroids. For asteroids diffuse reflection is the relevant process for incoming infrared radiation, where incident rays are reflected at many angles, rather than at just one angle as in the case of specular reflection (Wang et al., 2004).

Infrared radiation (IR) has longer wavelengths than those of visible light (0.7–500 μm = 14000-20 cm^{-1}), including the most important range for analytical chemistry between 50 and 2.5 μm (200-4000 cm^{-1}), while 15.4–7.7 μm (650-1300 cm^{-1}) is called fingerprint region. The infrared spectroscopy is based on the interaction of infrared radiation and matter and able to identify chemical bonds in a molecule, depending on the types of interaction (e.g., transmission, reflection) between the sample and the IR radiation.

Infrared absorption peaks correspond to the frequencies of vibrations between bonds of atoms. Thus the absorption bands at different wavelengths or wavenumbers are characteristic for specific material and allow the identification of minerals of meteorites and asteroids. The detection capabilities of the near-infrared (VIS-NIR, 0.4–2.5 μm) and the less frequently used mid-infrared (MIR, 2.5–25 μm) ranges are slightly different. The VIS-NIR (0.4–1 μm) region is especially important for iron-oxide identification. The NIR region (1–2.5 μm) is fundamental in identifying and discriminating between micas, chlorites, carbonates and clay minerals, through its ability to detect hydroxyl and carbonate bond related vibrations. In the MIR region many fundamental absorption features related to OH bonds occur, and provide possibility for identification of tectosilicates, oxides and sulphide minerals (Morlok et al., 2010). Spectral libraries support the interpretation of IR spectra (Donaldson Hanna et al., 2012).

Analysis of different **meteorites** and meteorite minerals is important to get information on the surface characteristics of asteroids. The most common minerals of undifferentiated meteorites are olivine, pyroxene and plagioclase feldspar. Their distinct and strong spectral features may be slightly distorted by contaminating H_2O, but the IR peaks often help to distinguish between different types of them (Salisbury et al., 1991) (for specific values see the Results section). Understanding of peak positions was improved by the analysis of synthetic minerals (Hofmeister and Pitman, 2007). Detailed correlations of composition with spectral characteristics have been described for main meteorite minerals like olivine or pyroxene (Hamilton, 2000a; 2000b). Among the carbonaceous chondrites CI and CM groups showed variability in the shape of the silicate features related to the increasing extent of aqueous alteration (Beck et al., 2014). The broad absorption feature in the 10-13-μm region of CM/CI meteorites is due to Mg-rich phyllosilicates and unaltered olivine (McFadden et al., 2015), its changes with total phyllosilicate abundance from shorter in less altered meteorites to a longer wavelength in the highly altered meteorites. Comparing the visible to near-infrared (VNIR) and thermal infrared (TIR) spectral ranges the differences between the mineral mixtures and surveyed meteorites could be identified. They arise from the differences in the types and physical disposition of constituents, and also from albedo differences (Donaldson Hanna et al., 2019). In meteorite spectra the most significant absorption band is often the O–H stretching vibration feature and the H–O–H bending vibration when molecular water is present (Salisbury et al., 1991). The later **water content** might emerge in different crystalline positon, could be even not embedded in the mineral lattice. Especially this later could be an artefact from the observing conditions in Earth laboratories if the sample is not preheated (Góbi et al., 2014).Similar spectral features also can derive from hydrous magma or different types of fluids and might exist in minerals at structural defects or as fluid inclusions. Absorption features in the MIR related to O–H stretching vibration emerging in the spectra around 3000-3500 cm^{-1}. Crystalline water produces band about 3400–3650 cm^{-1}, solid ice also appears about 3200–3600 cm^{-1}, and adsorbed water band appears about 3700–3800 cm^{-1}.

Beside the above listed findings, the **reference data** for analysis of minerals based on infrared spectra are also useful as background, and should be used during the planning of instruments and interpretation of results. A summary of the largest database is given in Table 1. The results presented in this work are often less detailed (for example in spectral resolution or target material component information) than these databases, in order to demonstrate which aspects should a simple IR detector focus on for mineral identification in the future of asteroid exploration.

While the above listed databases are highly useful, they might be further developed to ideally support the interpretation of asteroid spectral observations expected to be gained in the near future. For example, in the known infrared spectral databases there are few spectra of mineral and meteorite mixtures (powder-powder mixture, or different grain size powders or powder-chips mixtures), as in the case of real asteroids mixtures might be present. There are only a few mineral spectra which are measured at different temperatures (in SSHADE). In the NASA JPL Ecostress and USGS spectral databases most of the measured meteorites are fine grained, there are no single different (larger) grain size meteorite spectra. These aspects suggest it is worth evaluating further laboratory tests to enlarge the range of reference data types.

1.1.1. *Asteroid spectral taxonomy*

Several taxonomy systems have been published to classify asteroids using the optical and infrared spectral properties. Chapman et al. (1975) developed a relatively simple taxonomic system based on colour, albedo, and spectral shape, classifying the asteroids to “C" for dark carbonaceous (C), stony (S), other as “U" class (that did not fit into either C or S). This classification has since been expanded and improved, and various other systems have been also proposed. Widely used is the Bus-DeMeo asteroid taxonomy classification, described in DeMeo et al. (2009), and presented online as DeMeo 2009. It is based on the reflectance spectral characteristics of 371 asteroids recorded between 0.45 and 2.45 μm. It established 24 classes based on principal component analysis, following the visible wavelength based taxonomy of Bus et al. (1999), which itself supported by the earlier Tholen (1984) system. The Small Solar System Objects Spectroscopic Survey (S3OS2 or Lazzaro classification, Lazzaro et al., 2004), grouping 820 asteroids, also uses the Tholen and Bus–Binzel taxonomy. The SMASS classification (Bus et al., 2002a, 2002b) is also closer related to these earlier ones, classifying 1447 asteroids, and using also narrower spectral features than before. The improvement of classification systems (DeMeo and Carry, 2013) is based on the increasing number of observations, the increase of covered range and improvement spectral resolution. The latest (and next expected) improvements will cover the middle- and far-infrared ranges too, where more compositional data is expected to be gained – this work is to review the observational possibilities related to this less exploited range.

1.1.2. *Telescopic asteroid spectral observations*

Infrared observations of **asteroids** have been utilized for a long period, first mainly for size estimation with the help of albedo determination (Harris, 1998), and recently also for the estimation of regolith properties and composition (Clark et al., 2002). In the thermal infrared region (5–30 μm) fundamental modes of silicate Si–O bounds are present, providing information complementary to the visual and near-infrared regions. Observations from the Earth surface using infrared techniques are limited by atmospheric absorption, although there is an atmospheric window at 5–20 μm, which shows important mineral features. However, many telluric absorption bands are present in this region partly from ozone, carbon-dioxide etc., and the sky itself is bright due to thermal infrared radiation from the atmosphere, increasing the noise level. Another reason for the generally poor spectra is the space weathering of asteroid surfaces (Noguchi et al., 2011).

Asteroid mineralogy has mainly been based on **visible to near-infrared spectroscopy**. Certain mineral species display diagnostic near-infrared absorption features (e.g. pyroxene ~1 and ~2 μm, see Gaffey et al., 2002), but not all of the major minerals. For example, the silicate minerals thought to be the main constituents of asteroid surfaces have major Si–O stretching bands in the 10 μm region. Particular types of

Table 1
Summary of the five largest databases that contain infrared spectral data of minerals. Comments: *includes data from three other spectral libraries: Johns Hopkins University (JHU), Jet Propulsion Laboratory (JPL), United States Geological Survey (USGS - Reston).

Name	Measurements	Samples included	Accessible data types	Website URL
RELAB	NUV, VIS, NIR bidirectional spectrometer and NIR, MIR FT-IR spectrometer.	rocks, minerals, soils, biological, synthetic	spectra, modal mineralogy,	http://www.planetary.brown.edu/relab/
ECOSTRESS (former ASTER)*	VNIR, SWIR, TIR, directional hemispherical reflectance, bidirectional reflectance (2.08–25 μm)	mineral, rock, manmade, soil, lunar, meteorite, vegetation	spectrum, ancillary (sample type, class, subclass, particle size, wavelength range, origin, owner, description, XRD analysis)	https://speclib.jpl.nasa.gov/
ASU	thermal emission spectrometer (TES)	range of natural minerals	spectrum, description information (composition, sample source, quality, visual inspection results, bulk ox-ides, microprobe oxides, X-ray diffraction analysis results, and particle size)	http://tes.la.asu.edu/
USGS Spectral Library	spectral reflectance, UV-VIS-NIR, MIR, FIR	minerals, soils, coatings on rock surfaces, liquids, organics, synthetic materials, biological materials	spectra, detailed sample descriptions (results of XRD, EPMA, and other analytical methods)	https://www.usgs.gov/labs/spec-lab
SSHADE	range of instruments, including optical, infrared an X-ray data	ices, minerals, rocks, organic and carbonaceous materials, synthetic materials, liquids	spectra, ancillary data, detailed information on used instruments and measurements	https://www.sshade.eu/

minerals (e.g. the plagioclase feldspars) have useful diagnostic features only in the MIR (Lim et al., 2005). Among the most important **mid--infrared spectral features** there are 1. the Christiansen feature due to a transition between the surface and volume scattering regime (Hapke, 1996), appearing as a reflectance minimum at about 7.5–9 μm in the case of silicates, 2. the Restrahlen bands arise from fundamental molecular vibrations as most incident radiation does not enter the sample but is reflected at the first surface, resulting in a peak in the reflectance at about 8.5–12 μm by Si–O asymmetric stretching (however a less intense Restrahlen band appears around 16.5–25 μm) and 3. Transparency feature is located between two Restrahlen bands in the spectra of particulate silicates as a broad reflectance maximum and dependent on the presence of small particles (<75 μm) and changing optical constants. These features are diagnostic of the given mineral (e.g. Logan et al., 1973; Salisbury et al., 1991). It is also advantageous, that main-belt asteroids, having surface temperatures between 200 and 300 K, emit thermal radiation with spectral peaks in the 10–20 μm region. Thus mid-infrared spectroscopy has the potential to complement the visible to near-infrared data in asteroid exploration (Takahashi et al., 2011). Early reports of mid-infrared spectroscopy of asteroids were published by Gillett and Merrill (1975), Hansen (1976), Feierberg et al. (1983), and Green et al. (1985), while Cohen et al. (1998), Dotto et al. (2000), Lim et al. (2005) and Vernazza et al. (2010, 2012) established the modern mid-infrared (5–14 μm, 5.8–11.6 μm, 8.2–13.2 μm) spectroscopy of asteroids.

Analysis **of surface mineralogy of asteroids** enables the identification of several meteorite parent bodies in the main asteroid belt, and the determination of mineral chemistry and abundance in different meteorite types. Ground-based characterization of small bodies, with the SpeX instrument in the NASA Infrared Telescope Facility (IRTF) on Mauna Kea Hawaii enables the mineralogical characterization of asteroids down to visual magnitude of 19 (Reddy et al., 2015). In addition to ground-based observations there were a series of successful spacecraft missions, like flybys of (2867) Steins, (21) Lutetia, (4129) Toutatis, (4) Vesta and (25143) Itokawa. These missions provide data about the shape, morphology and surface composition of these asteroids (Reddy et al., 2015). With the Spitzer Space Telescope the Christiansen, the Restrahlen, and the Transparency features were also detected for asteroids (2867) Steins and (21) Lutetia (Barucci et al., 2008). Based on recent results, even small asteroids seem to be covered by regolith and optical changes occur along with the exposure of regolith by UV and ionizing irradiations driven maturation process. Infrared measurements were often used for **thermal inertia** calculation to allow the estimation if the surface layer consists of loose or consolidated surface material (Campins et al., 2009).

Important new results also emerged by the MIR studies by the **Spitzer Space Telescope**, mainly on the physical characteristics like diameter, albedo and thermal inertia of asteroids (Mainzer et al., 2015). Spitzer IRS spectra (5–38 μm) revealed broad emission features near 10 and 20 μm on three Jovian Trojans, pointing to the presence of fine-grained silicates (Emery et al., 2006), just like the plateau between 9 and 12 μm on eight Themis-family asteroids and (65) Cybele (Licandro et al., 2011). The far IR/submillimetre region also been used to constrain volatiles like water vapour around Ceres approaching the perihelion (Kuppers et al., 2014). In the case of asteroid (16) Psyche the MIR spectra pointed to metal rich bedrock surface and fine grained silicates (Landsman et al., 2018). Thermal analysis of the binary Trojan asteroid (617) Patroclus-Menoetius pointed to the existence of fine grained regolith cover composed of silicates based on emissivity features near 10–20 μm as in many Trojan asteroids (Mueller et al., 2010; Emery et al., 2006).

The 8-12-μm mid-infrared spectra of (24) Themis and (90) Antiope recorded by Spitzer pointed to (90) Antiope lacking a dusty surface, in contrast to other Themis family members (Hargrove et al., 2015) or (21) Lutetia (Lamy et al., 2010). For Themis family members the survey of the 10-μm silicate emission suggests these asteroids resemble meteorites with low abundances of phyllosilicates (Landsman et al., 2016). The MIR spectra of asteroid 956 Elisa showed a range of spectral features, including 9–12 μm and 16–25 μm Reststrahlen bands (pointing to diegenitic pyroxenes), and the 15–16.5 μm Si–O–Si stretching, while spectral deconvolution of the 9–12 μm Reststrahlen features indicates up to 20% olivine is also present (Lim et al., 2011). In addition to asteroids, the Mid-infrared spectral range has been observed in comets. For example, MIR mineral observations revealed amorphous and crystalline silicates, amorphous carbon, carbonates, phyllosilicates, polycyclic aromatic hydrocarbons, water gas and ice, and sulfides in the infrared spectra of the ejecta of comet 9P/Tempel 1 during the Deep Impact event (Lisse et al., 2006).

Space weathering also influences asteroid spectra, causing darkening (Harris et al., 2009). Based on Vernazza et al. (2010) variability in the MIR spectra is strongly influenced by space weathering effects beside grain size, although surfaces are often covered by very porous materials (Vernazza et al., 2012). During space weathering the amorphisation of

silicates causes a shift of the 10 μm feature to longer wavelength, found by irradiation tests of the Tagish Lake meteorite (Vernazza et al., 2013). The laboratory simulation of solar wind irradiation of meteorites produced a shift of the phyllosilicates (about 3 and 10 μm) and silicates (about 10 μm) bands toward longer wavelengths (Lantz et al., 2017). Another project simulated solar wind implantation of carbonaceous chondrites, and identified modification of adsorbed water content, phyllosilicates and organic material too, and shift of the 9.9 μm silicates band probably due to a preferential loss of Mg (relatively to Fe) or by amorphisation of Mg-rich minerals (Lantz et al., 2015). They also indicated that the reddening/darkening trend for carbonaceous chondrites depends on the initial albedo. Another laboratory test with Allende CV3 chondrite and eucrite NWA 6966 meteorites pointed to a decrease of infrared reflectance and overall spectral reddening possibly caused by interplanetary dust impacts (Fiege et al., 2019).

1.1.3. Close-by asteroid spectral observations

Spatially resolved infrared spectral observations of recent missions highlighted the importance of nearby spectral analysis from orbiters and landers (Hamm et al., 2018), presenting a range of details, which could not have been identified form far away. The boulder covered surface of the C-type asteroid **Ryugu** was imaged by the Hayabusa-2 mission (Michikami et al., 2019). At global scale Ryugu' spectra seems to be flat, with red slope (Sugimoto et al., 2019).The spectra showed few characteristic features, among them the 2.72 μm band emerged at many locations of the surface (Riu et al., 2019), suggesting an OH component, possibly from phyllosilicates. Comparison of the recorded spectra to those of various carbonaceous chondrite meteorites (CM/CR/CI) suggests that the material of Ryugu, although being hydrated, experienced a certain level of heating and partial dehydration (Nakamura et al., 2019). Based on thermal images from the TIR camera, most boulders in close-up analysis showed temperature similar to the surroundings on average, but with more variability probably due to the different insolation geometry and thermal inertia (Okada et al., 2019).

The observations by the OSIRIS-REx of (101955) Bennu NEA, revealed a carbonaceous surface covered by fine-grained (sub-cm) regolith with bright decameter-scale boulders (Rizk et al., 2019). It is having generally a low thermal inertia (Emery et al., 2019) with increasing thermal inertia along with the albedo (Rozits et al., 2019a). Few and small hazard-free surfaces were found (Lauretta et al., 2019) including the equatorial area where fine grains have been suggested earlier (Binzel et al., 2015). The asteroid has a low cohesion, rubble pile interior (Barnouin et al., 2019). Spectral analysis revealed abundant hydrated minerals on its surface (Hamilton et al., 2019), with absorption near 2.7 μm and thermal infrared features similar to those of aqueously altered CM-type carbonaceous chondrites of petrologic types 1–2, while a spectral feature at 440 cm^{-1} (~22.7 μm) points to phyllosilicates, although heating might have also influenced the body (de León et al., 2018). Parts of Bennu's surface could have become blue due to space weathering, while fresher areas are redder (Lanzt et al., 2018).

2. Methods

This section provides an overview of the DRIFT based infrared method including the specific instrumental setup used for the recording of spectra by the authors. This papers focuses on the middle infrared region to support the planned future asteroid observations by helping in the fine adjustment of detector design, observational planning and targeting the data acquisition. DRIFTs (diffuse reflectance infrared Fourier transform spectroscopy) is an **infrared sampling method**, using a complex process, which covers absorption, transmission, internal reflection, specular (regular and Fresnel type) reflections and diffusion. DRIFTs is mainly used to analyse powders and solid samples (Fuller and Griffiths, 1978), and the recorded spectra primarily serve the purpose of **qualitative analysis**, but it also provides **quantitative information** using the characteristic bands. The specific properties of the material influence the quality of the DRIFT spectrum: refractive index of the sample, grain size, packing density, homogeneity, concentration and also measuring conditions (Armaroli et al., 2004).

The **DRIFT instrument** operates by directing the IR radiation into a sample cup, where it interacts with the grains, gets reflected off their surfaces, causing the light to diffuse or scatter, as it moves throughout the sample (Drochner and Vogel, 2012). The IR radiation is reflected on the sample surface in all directions, therefore DRIFTs requires a special mirror arrangement (Fraser and Griffiths, 1990; Korte, 1990; Kortüm and Delfs, 1964; Mitchell, 1993). The output mirror then directs this scattered radiation to the detector in the spectrometer to record the altered IR beam as an interferogram signal, which can then be used to generate a spectrum. Typically, a background is collected with the DRIFTs accessory in place and the cup is empty or filled with just KBr material.

The **reflection on sample surfaces** or powdered samples is subdivided into different categories (Mitchell, 1993). There are external (reflection of radiation on surfaces) and internal (the reflection occurs at the border between two condensed phases) reflections. For external reflections, there are specular and diffuse types. Reflection at boundary layers are not oriented parallel to the "macroscopic" surfaces. The single and multiple reflections thereby lead to a diffuse component of Fresnel reflection. Reflection on rough surfaces produces diffuse reflection. In contrast to the simple specular reflection, diffuse reflection has no definite orientation. The Fresnel type reflection can influence the resolution by smearing out the bands by the Fresnel reflection and cause the shift or distortion of particular bands. The diffuse and specular reflections are not optically isolable, therefore diverse models exist for the quantitative description of diffuse reflection (Dahm and Dahm, 2007; Gade et al., 1987; Hecht, 1976; Kortüm, 1969; Mandelis et al., 1991; Melamed, 1963; Simmons, 1975); the most commonly used is the Kubelka-Munk model (Smith, 2011).

For useful measurements the **grain size** must be smaller than the wavelength of the incident IR radiation (MIR region <5–10 μm), what might be a potential problem that small asteroids surfaces seem to be dominated by larger grains. **Temperature** also influences the position, width and intensity of bands in the spectrum. With increasing temperature the bands get broader and weaker, some bands are lost, and all the bands are usually shifted to longer wavelengths. These effects are due to diffusion of the infrared beam on the sample, which increases with increasing temperature and the signal-to-noise ratio decreases accordingly (Armaroli et al., 2004).

Although DRIFT is useful for quality analysis of minerals, it is worth mentioning that it is not ideal for quantitative analysis, and this method also introduces artefacts in the band shapes due to polarisation and orientation effects, however this effects could be partly corrected. In the DRIFT spectrum there is no linear correlation between band intensity and concentration, however the Kubelka-Munk expression (Wendland and Hecht, 1966; Kortüm, 1969; Kubelka and Munk, 1931; Kubelka, 1948; Hecht, 1980) makes a linear approach between the spectral intensity and sample concentration. Mid-infrared (2.5–25/μm) reflectance spectra of minerals are sometimes used to predict emittance qualitatively through Kirchhoff's law. These spectra display weak overtone and combination tone bands, which may be as diagnostic of composition as the strong fundamental molecular vibration bands usually considered for remote sensing applications (Salisbury et al., 1987), while the emission spectroscopy technique allows for direct, quantitative comparison of laboratory spectra to remote sensing data sets (Christiansen et al., 2000).

For our measurements we used a DRIFTs instrument, which is connected to a Vertex **FTIR 70** infrared spectrometer, and composed of a Praying Mantis diffuse reflectance accessory and a reaction chamber with tuneable temperature (−150 … +600 °C) – however several measurements listed here have been done at room temperature. The measurements usually were performed with the following parameters: spectral resolution: 0.04 μm (4 cm^{-1}), number of scans: 256, covered wavelength range: 2.5–25 μm (4000-400 cm^{-1}). Before the measurements the meteorite materials were grinded down to 10–50 μm diameter powder,

and dried by keeping them at +120 °C for 12 h in the oven.

To get a general overview of spectral characteristics in the MIR region powders of four meteorites were analysed (Table 2): NWA 869 is an L4-6 chondrite, Jiddat al Harasis 055 (JAH 055) is also an L4-5 chondrite (examples of the most common ordinary chondrite type), and the NWA 11469 is a CO3 and Allende is a CV3 type carbonaceous chondrite, also relatively common meteorite. All samples were grinded to fine powder size with most grains below 20 μm to gain good quality spectra in the middle infrared range, however in reality larger grains on small asteroids might require further developed of simulants. To support the mineral interpretation, pure olivine, pyroxene, and feldspar standard samples and literature based references were also used in this work.

Control measurements using powder diffraction method was also applied to have an independent estimation on the mineral composition of analysed samples. For XRD measurement's we used Rigaku Miniflex600 Bragg-Brentano powder-diffractometer. We milled 40 mg of the samples mixed it with 1.5 ml ethanol and dry it on a steel section to gain the XRD sample. In Miniflex600 the X-ray source is Cu, we used 40 keV accelerating voltage and 20 mA beam current. There is a scintillation detector NaD graphite monochromator, and the measurement time is 35 min.

3. Results

Section 3.1 gives an overview of related earlier results firstly in the NIR, secondly in the MIR regions. Section 3.2 explains the laboratory based observations made by the authors, followed by an evaluation of the role of grainsize (3.3) and temperature (3.4). The observational relevance and possibilities are discussed in the 4th section.

3.1. Summary of band positions

Below we present the characteristics of the main minerals first (to see the possible bands and targets for a mid infrared analysis), after this those parameters are selected and listed, which might be observable by a future mission in the MIR region. Finally, an overview of the grain size related characteristics of the visited asteroids is given, as they might have substantial influence on the observability.

3.1.1. Near infrared region

Earlier works focused more on the **near-infrared region**, thus it is important to see the similarities and differences between the two regions. In the near-infrared spectrum of **olivine** with increasing temperature the ~1 μm band, produced by ferrous iron (Fe^{2+}), broadens (mainly on the long wavelength side), so the FWHM is increasing (Hinrichs et al., 2002; Singer and Roush, 1985) and the observability of the fine scale structure is decreasing, while with decreased temperature, the ~1 μm band become better resolved and shows changes in relative absorption strength (Singer and Roush, 1985).

Pyroxene near-infrared spectra display two well-defined Fe^{2+} absorption bands near 1 and 2 μm (Adams, 1974). Both ortho- and clinopyroxene spectra display significant changes in band symmetry with temperature, showing the same trend of broadening of the 1- and 2 μm bands (so their FWHM is increasing), especially at the longer-wavelength edge, while the position of the near 1 μm absorption band remains unchanged over a wide temperature range (80–448 K) (Hinrichs et al., 2002; Singer and Roush, 1985). In contrast, the 2 μm absorption band shifts in different directions: in orthopyroxene it shifts to longer wavelength with increasing temperature, while in clinopyroxene it shifts to shorter wavelength (Singer and Roush, 1985; Corley and Gillis-Davis, 2015). Based on the work of Roush (1984) the spectra of plagioclase are suggested to be relatively independent of temperature.

3.1.2. Middle infrared region

Surveying the **middle infrared region**, the most common mineral on stony asteroids based on meteoritic evidences is **olivine**, a complete solid solution of minerals ranging from magnesium-rich forsterite to iron-rich fayalite. The composition is usually expressed as the molecular percentage of fayalite (e.g., Fa_{30}); the remaining percentage of forsterite is assumed as if no other minerals beyond these two were present. Magnesium-rich olivines are much more common in primitive meteorites and asteroids than iron-rich olivines (Sunshine et al., 2007), the latter are more abundant in thermally processed meteorites. Olivine composition is an important factor during the classification of meteorites and asteroids (Mason, 1968) and it can serve as an indicator of the formation processes or conditions of a meteorite or asteroid (Sunshine et al., 2007). Olivine is characterized by several main absorption bands listed in Table 3 (Burns and Huggins, 1972; Duke and Stephens, 1964; Iishi, 1971; Lane et al., 2011; Reynard, 1991; Salisbury et al., 1991). Amorphous olivines have broad absorption features near 10 μm and a weaker band at about 20 μm (Day, 1981).

Pyroxenes are another main components of meteorites. Based on composition there are **low ($Fs_{0.1}$-$Fs_{41.5}$)** (Fs: ferrosillite) **and high-calcium ($Fs_{1.8\text{-}35.2}$ $Wo_{44.4\text{-}61.0}$)** (Wo: wollastonite) **pyroxenes** (LCPs and HCPs, respectively). Based on previous publications (Chihara et al., 2002; Cloutis et al., 2013; Mason, 1968; Salisbury et al., 1991) the most common pyroxene minerals in meteorites belong to the clinoenstatite-clinohypersthene series, mainly enstatite, diopside, bronzite, pigeonite and augite.

The **FeNi minerals (kamacite, taenite)** are frequent in meteorites but are not observable in the MIR region, because metals do not absorb IR radiation or display bands only in the FIR region (25–1000 μm) (Belskaya et al., 2012; Reichenbächer and Popp, 2012). These minerals might have a small influence of the shape of visible and near infrared spectra (0.2–2.6 μm), and provide a reddish spectral contribution to many asteroids (Gaffey et al., 1993).

3.2. Laboratory measurements

In this section we outline infrared spectra of four meteorites in order to evaluate, how much the above discussed characteristics could be identified. The resulting spectra (Figs. 1 and 2) show the main components with the indicated peaks of the three main minerals: olivine, pyroxene and feldspar. As it is visible, in several cases the same peaks of the same minerals were observed. The identified peak positions are: olivine (11.86, 11.93, 16.31, 16.61, 19.72 μm, e.g. 843, 838, 613, 602, 507 cm^{-1}), pyroxene (9.77, 11.57, 19.88, 20.66, 21.32, 22.32 μm, e.g. 1023, 864, 503, 484, 469, 448 cm^{-1}), feldspar (8.71, 9.22, 13.75, 15.38, 17.76, 18.72, 21.18, 23.69 μm, e.g. 1148, 1084, 727, 650, 563, 534, 472, 422 cm^{-1}).

Table 2
Modal mineralogical composition of the measured meteorite samples using powder diffraction method.

JAH 055			Allende			NWA 869			NWA 11469		
Mineral		%	Mineral		%	Mineral		%	Mineral		%
Olivine	Forsterite	42	Olivine	Forsterite	69	Olivine	Forsterite	41	Olivine	Forsterite	51
	Fayalite	1.2		Fayalite	2.6		Fayalite	6		Fayalite	7
Feldspar	Anorthite	18	Feldspar	Anorthite	2.3	Feldspar	Anorthite	16	Feldspar	Anorthite	1.7
Pyroxene		31	Pyroxene		24	Pyroxene		35	Pyroxene		8.3
Goethite		0.5	Goethite		0.3	Goethite		0.3	Goethite		28
Troilite		8	Troilite		1.5	Troilite		2.1	Troilite		4

Table 3
Main IR peak positions of major meteorite minerals and their variation with chemical composition. The indicated peaks were selected as the most obvious ones, and might include Reststrahlen and Christiansen features. Used references: Chihara et al. (2002); Cloutis et al. (2013); Jäger et al., (1998); Koike et al., (1993); Nash and Salisbury (1991); Salisbury et al. (1991).

Minerals	General peak positions (μm)	Further specific peak characteristics
olivine	in the 4.9–5.9 μm and 10.4–12.2 μm regions, mainly: 11.5, 10.5, 10.2, 9.5*	• reflectance plateau at 10.5–11.5 μm, two smaller, rounded peaks at 9.5 and 10.2 μm, • systematic shift to longer wavelengths as the Mg content decreases and Fe content increases.
pyroxene	5.1, 5, 4.5**, 9.77 10.3, 11.57, 14.77, 14.94	• low-Fe^{2+} LCP: near 4.8 and 5.1 μm, • most bands shifted to longer wavelengths with increasing Fe concentration, the 4.8 μm band transforms to an inflection point, but some peaks (e.g. 9.9, 13.6 μm) do not shift or shift to shorter wavelengths (e.g. 10.7, 11.7 μm).
plagioclase feldspar	5.4, 4.8, 4.7***, 13.75 15.5	• albite shows two weak absorption bands near 4.8 and 4.9 μm • anorthite (An):strongest band near 5.4 μm, • peaks often weaken and shift to longer wavelength with increasing An content. • the lowest An content samples display the most absorption features, without systematic spectral changes with composition, • plagioclase feldspars in meteorites are mostly An rich and with two main bands at 4.73 and 4.82 μm, an inflection near 4.93 μm and weak bands near 4.35, 4.45, and 4.65 μm.

The two reflectance spectra in Figs. 1 and 2 provides example for the general appearance of main minerals of two typical meteorites. For NWA 869 (Fig. 1) powder diffraction based compositional analysis have been also done, and gave forsteritic olivine (41%), pyroxene (35%) and plagioclase feldspar (16%) with a few fayalitic olivine (6%), troilite (2.1%) and goethite (0.3%) as main components. For NWA 11469 (Fig. 2) the powder diffraction based compositional analysis gave forsteritic olivine (51%) and goethite (28%) with a few pyroxene (8.3%), fayalitic olivine (7%), troilite (4%) and plagioclase feldspar (1.7%) as main components. The composition from powder diffraction based analysis confirmed the infrared results. Of course space weathering would decrease and weaken various infrared peaks, making difficult the identification, but the evaluation of this effect is beyond the scope of this paper.

3.3. Role of grain size

Grain size also effects the spectra as the strength of Reststrahlen features changes inversely proportionally to particle size (Le Bras and Erard, 2003). With increasing **grain size,** the reflectance decreases, absorption bands become weaker (Cloutis et al., 2013; Salisbury et al., 1987; Salisbury and Walter, 1989) and the apparent loss of spectral detail becomes observable (Fig. 3). The mineral composition using powder diffraction for the Allende meteorite gave as mainly forming minerals: forsteritic olivine (69%) and pyroxene (24%) with a few fayalitic olivine (2.6%), plagioclase feldspar (2.3%), troilite (1.5%) and goethite (0.3%) – also in agreement with the infrared analysis. Grain size also changes the depth and slope of the absorption features. Spectral slope is measured as the dependence of reflectance on wavelengths, it is typically expressed in percentage increase of reflectance per unit of wavelength (%/100 nm). The red slope means the increase of reflectance with wavelength, while blue slope means that reflectance is decreasing with wavelength. In the infrared spectra larger grain size typically means deeper bands and blue (more negative) spectral slope in the visual range (Reddy et al., 2015), so in case of large grain size the reflectance will decrease with wavelength. Based on Bus et al. (2002) the B, K and L type asteroids display slightly bluish slope, the C, X, T, Q and O type asteroids display moderate reddish slope, while the D, A, R and V types show very steep red slope (SMASSII asteroid classification).

To estimate the probable grain size to meet on Didymos and its moon, the following earlier results could be considered. Based on Nakamura et al. (2011) the analysis of grains returned by the Hayabusa-1 spacecraft from the near-Earth asteroid (25143) Itokawa have shown that a majority of grain sizes is 3–40 μm, and most of them are smaller than 10 μm – however the sampling process was not regular and the data from Itokawa need not be representative. Thus the spectra of meteorite samples with grain sizes <100 μm would best represent the spectra of asteroid regolith (Reddy et al., 2015), possible except for the small asteroids.

Samples with smaller average particle sizes (<10 μm) give better spectra with reduced peak widths (FWHM) compared to samples with large average particle sizes (>90 μm) (Fuller and Griffiths, 1978). An

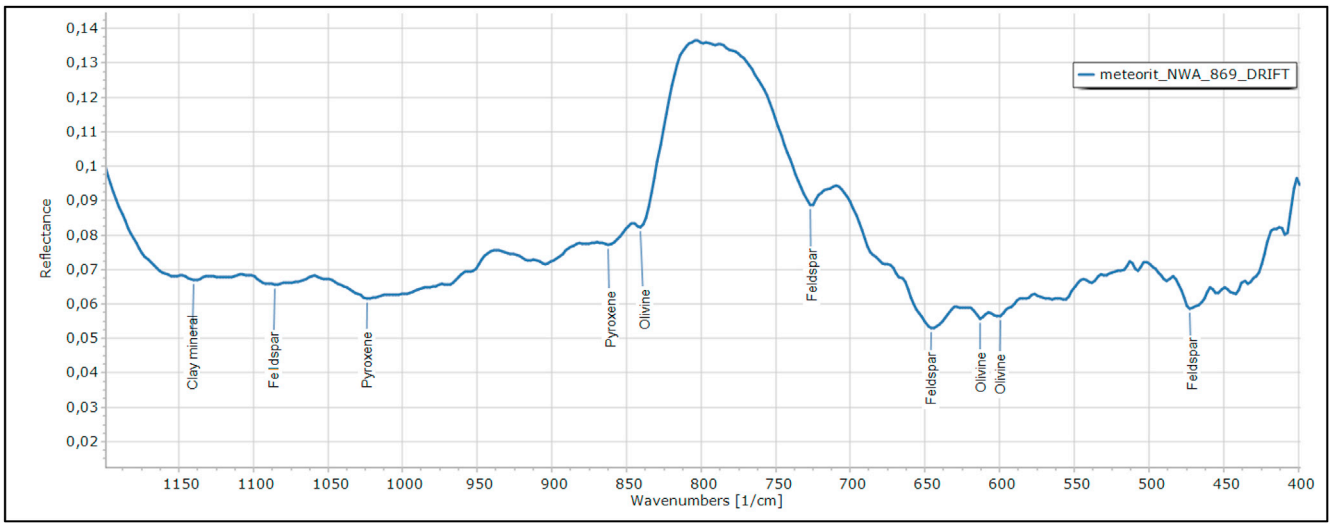

Fig. 1. Bands of main minerals in the reflectance spectrum (8.33–25 μm, 1200-400 cm^{-1}) of NWA 869 fine meteorite powder.

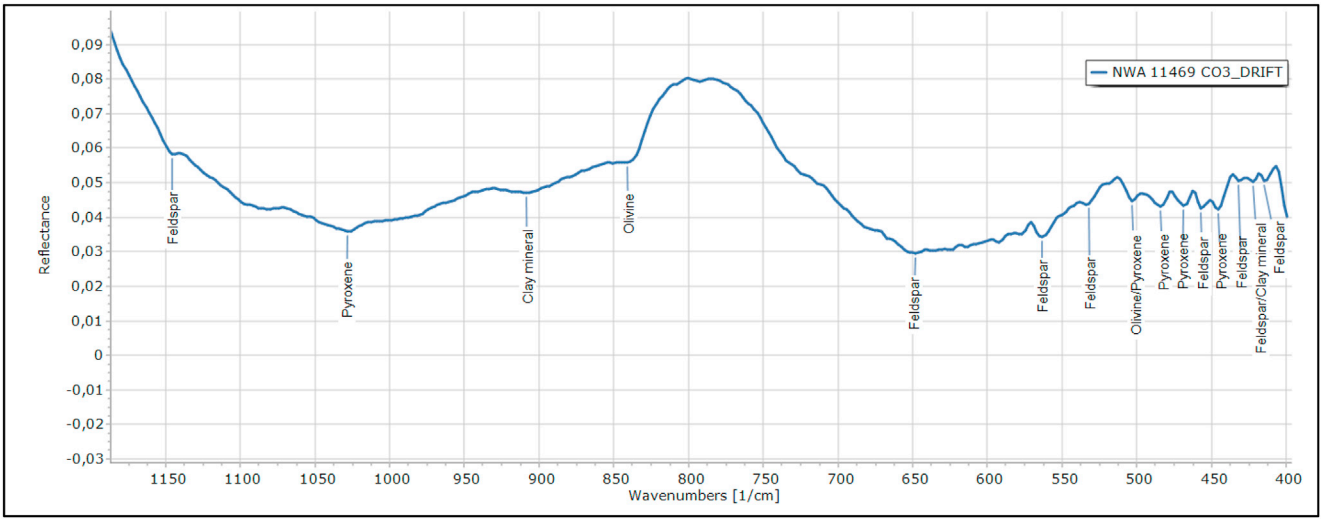

Fig. 2. Bands of main minerals in the reflectance spectrum (8.33–25 μm, 1200-400 cm^{-1}) of NWA 11469 fine meteorite powder. Based on powder diffraction measurements the NWA 11469 meteorite is mainly forming from.

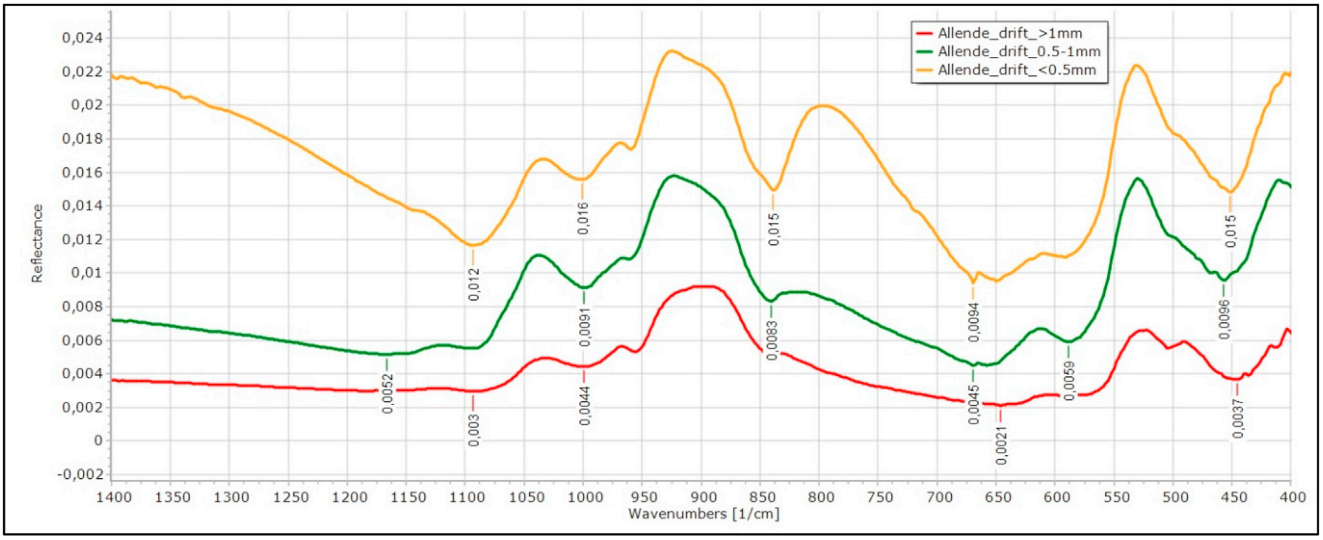

Fig. 3. Diffuse reflectance spectra of different grain sized meteorite powders of Allende CV meteorite. The three curves represent >1 mm, 0.5–1 mm, 2–50 μm sized grains. In the diagram the curves upward show smaller grain sized spectra with higher reflectance values.

average particle size of 10 μm is appropriate for quantitative measurements of powders, while 50–100 μm can be good for qualitative analysis (Thompson and Palmer, 1988). In this work the authors are interested in to evaluate more the realistic than the ideal (from the point of view of spectral feature identification) grain sized sample – thus despite better quality spectra could be achieved by the finer powder here larger size diameter were considered, as asteroid surfaces show probable mixed grain size.

3.4. Role of temperature on infrared spectra

The **effect of temperature** on the infrared spectra was observed mainly in the VIS-NIR region (0.4–2.5 μm) (Hinrichs et al., 1999a, 1999b; Lucey et al., 2017; Roush, 1984; Roush and Singer, 1986; Singer and Roush, 1985). Based on previous studies both olivine and pyroxene spectra are sensitive to temperature changes, but there is a large difference between the two in terms of the wavelengths of greatest sensitivity (Hinrichs et al., 2002).

Based on the orbital characteristics of Didymos and selected end cases of thermal inertia values (50 and 1000) the surface **temperature** could be estimated for various latitude zones and local solar times on the asteroid. Although the exact temperature is unknown for Didymos, the expected temperature values were summarized in Table 4 below.

The temperature of the dayside of the asteroid surface can vary by as much as 100 K depending on the illumination. The variations in temperature produce a number of spectral effects, the reflectance spectra of several mafic silicates vary with temperature (Lucey et al., 2017, Roush, 1984; Roush and Singer, 1986; Singer and Roush, 1985; Moroz et al., 2000). The temperature effects the wavelength positions, shapes, and intensities of the absorption bands from Fe^{2+} in the reflectance spectra of mafic minerals (Roush, 1984; Singer and Roush, 1985; Roush and Singer, 1986; Schade and Wäsch, 1999, Hinrichs et al., 1999a, 1999b). A decrease in temperature reduces the amplitude of thermal vibrations of cations, resulting in a narrowing and shifting to shorter wavelengths of the absorption bands (Burns, 1970), so the identification of these bands becomes slightly easier.

In Fig. 4 the IR reflectance curves of JAH 055 L4-5 ordinary chondrite meteorite can be seen between +100 and −120 °C. Based on powder

diffraction measurements the JAH 055 meteorite is mineralogically mainly forming from forsteritic olivine (42%), pyroxene (31%) and plagioclase feldspar (18%) with fewer troilite (8%), fayalitic olivine (1.2%) and goethite (0.5%), in agreement with the infrared data. The infrared reflection curves resemble each other, along with the decreasing temperature the intensity of reflectance increases and the spectral details (fine structure of peaks) are more detailed. Peak shift also might emerge along with the temperature change, however its value is small, in the order of 1 cm^{-1} (0.01 μm) in the range shown in Fig. 4.

The observed differences related to different temperatures in the reflectance level were increased of less than 1% by 100 °C decrease, thus is not an important effect, especially compared to the grain size effect for example. Another consequence of the temperature is that colder sample and spectral recording provides less noisy spectra, however this effect was also not substantial, and was below 0,1% of reflectance. However his effect might be overcompensated by the gain in signal to noise ratio, as if the asteroid is brighter in thermal emission if the regolith is warmer.

4. Discussion

Based on the science case outlined above, the following observational possibilities are realistic, and the listed aspects should be the focus of future laboratory research to support asteroid missions and instrument design for close-by observations.

4.1. Expected observable features

While the analysis of laboratory spectra provides an easy and idealized way of mineral identification, the real life examples, like the cases of visited asteroids could be more complex and difficult to understand – here we use own observations and literature based data to have a broader picture. Early reports of MIR spectroscopy of asteroids were published by Gillett and Merrill (1975), Hansen (1976), Feierberg et al. (1983), and Green et al. (1985), while Cohen et al. (1998), Dotto et al. (2000) and Lim et al. (2005) established the modern MIR (5–14 μm, 5.8–11.6 μm, 8.2–13.2 μm) spectroscopy of asteroids. These observations provided some evidence for certain minerals, however no comprehensive discussion is available on the comparison of laboratory spectra to asteroids. Below we discuss the most relevant observable spectral features expected in asteroids, based on the analysis of meteorites. Although space weathering influences substantially the spectral characteristics, it is important to identify such marker spectral bands in laboratory analysis first, to be able to better understand the effect of cosmic weathering on complex asteroid spectra.

During the identification of main minerals (olivine, pyroxene, feldspar) the deepest and strongest peaks, which do not overlap with peaks of other known meteorite forming minerals and thus could be a **good indicator,** are listed below.

Based on the analysed meteorite spectra, for **olivine** the most characteristic peak is at 11.93 μm (838 cm^{-1}) with FWHM 0.09 μm (9.5 cm^{-1}), and less prominent ones are at 16.31, 16.52, 19.84, 24.09 μm (613, 605, 504 and 415 cm^{-1}). For **pyroxene** minerals the characteristic peak is at 9.77 μm 1023 cm^{-1} (FWHM ~0.01 μm = ~20 cm^{-1}) and less prominent ones are at 9.24, 10.3, 11.57, 14.77, 14.94, 20.66, 22.42 μm (1082, 970, 864, 677, 669, 484 and 446 cm^{-1}). **Feldspar** minerals have characteristic peaks at 13.75 (727 cm^{-1}) with FWHM ~0.002 μm–2.5 cm^{-1}, and another good candidate at 5.5 μm 645 cm^{-1} (FWHM ~0.02 μm–22.5 cm^{-1}) and less prominent ones are at 10.52, 16, 17.69, 17.18, 19.23, 21.18 μm (950, 625, 565, 582, 520 and 472 cm^{-1}).

Table 4
Model simulation based temperature values for Didymos and its satellite for perihelion and aphelion for its equator and at middle latitude terrane (Thermal inertia of the surface (Γ): 50 J m-2K-1s-½ (min), 1000 J m-2K-1s-½ (max), Bolometric Bond albedo of the primary: A = 0.07 ± 0.02, Emissivity: 0.9), ESA, M. Delbo).

	Perihelion (AU = 1.0131)				Aphelion (AU = 2.2754)			
	Γ = 50		Γ = 1000		Γ = 50		Γ = 1000	
	Day	Night	Day	Night	Day	Night	Day	Night
0°	391 K	165 K	340 K	265 K	250 K	130 K	200 K	190 K
60°	320 K	155 K	270 K	230 K	210 K	125 K	170 K	160 K

4.1.1. Expectations based on asteroids visited by spacecraft

Below the expectations are outlined for observational possibilities of asteroid IR spectra, focusing on the role of grain size and temperature. The **grain size** could influence several characteristics of asteroids, especially if it shows inhomogeneous spatial distribution. Based on Galileo observations, on the surface of Ida fresh craters show brighter, bluer, and deeper 1-μm absorption band than the rest of the surface (Sullivan et al., 1996). Comparing spectra of Ida with those of its satellite Dactyl, on the latter 1 μm absorption band is more dominant, interpreted as an increased pyroxene/olivine ratio or a coarser grain size of the regolith (Veverka et al., 1996). The 20–30 mm grain size on Itokawa expected from ground-based data was confirmed by the Hayabusa mission (Yano et al., 2006), but among the particles sampled by Hayabusa with unusual method that might influence the result, the acquired size ranged between 1 and 240 μm (Matsumoto et al., 2017), with many being smaller than 10 μm – although nominal sampling process probably would have provided different size distribution.

Based on the modelling of thermal inertia from remote observations, the regolith of asteroids is often dominated by relatively large mm-cm sized particles (Gundlach and Blum, 2013), for example the dominant average grain size is 20 mm for Itokawa (Nakamura et al., 2012), 1–3 mm on Eros (but also submillimetre on the smooth surface areas there, Robinson et al., 2002), 0.64 mm for 1998 WT24, 18 mm on 1999 JU3, 0.98 mm on 1996 FG3, 1.7 mm on Betulia, 12 mm on Elvira, 3.8 mm on Bohlinia, 0.028 mm on Herculina, 0.2 μm on Lutetia (the last 8 results are from Gundlach and Blum, 2013). On Gaspra the fresh craters show brighter and bluer appearance together with a deeper 1 μm band (Belton et al., 1996). As a summary, observations suggest there might be a trend regarding the dominant grain size: as the size of the asteroid and its gravity decreases the dominant grain size increases, thus bigger asteroids have smaller sized (or more smaller sized) grains, as expected based on the physical conditions. However, more data is necessary to confirm the trend.

The observed grain sizes range between > mm and some μm, thus such wide range of grain size might be present on many asteroids. The surface could be heterogeneous, for example for Bennu the best thermal models suggest the dominant grain size ranges between 1.2 and 31 mm (Yu and Ji, 2015), however several meter sized boulders are also present, often with fine-grained surface texture (Jawn et al., 2019). Considering this large range, based on our data and the related information from the literature, bands are fainter for larger grain sizes, while the peak position change is small, in the order of about 1 cm^{-1} (0.01 μm).

The **role of temperature** could also be identified using laboratory measurements, providing more detailed spectra with finer structure at lower than at higher temperature ranges. However the difference is small, is visible only if the spectral resolution is very high, in the order of about 1 cm^{-1} (0.01 μm). Spectra recorded at lower temperature regime support the detailed characterization of the target minerals while for the identification of main mineral types spectra at more elevated temperature might be sufficient.

The role of space weathering should also be considered during instrument design. Space weathering effects seem to decreases the depth of the 1 μm band (Adams and McCord, 1971), but there is less data available on this aspect in the MIR.

4.2. Instrument related aspects

Below the instruments related observational aspects are considered in order to see, which bands of certain minerals are possible to be observed

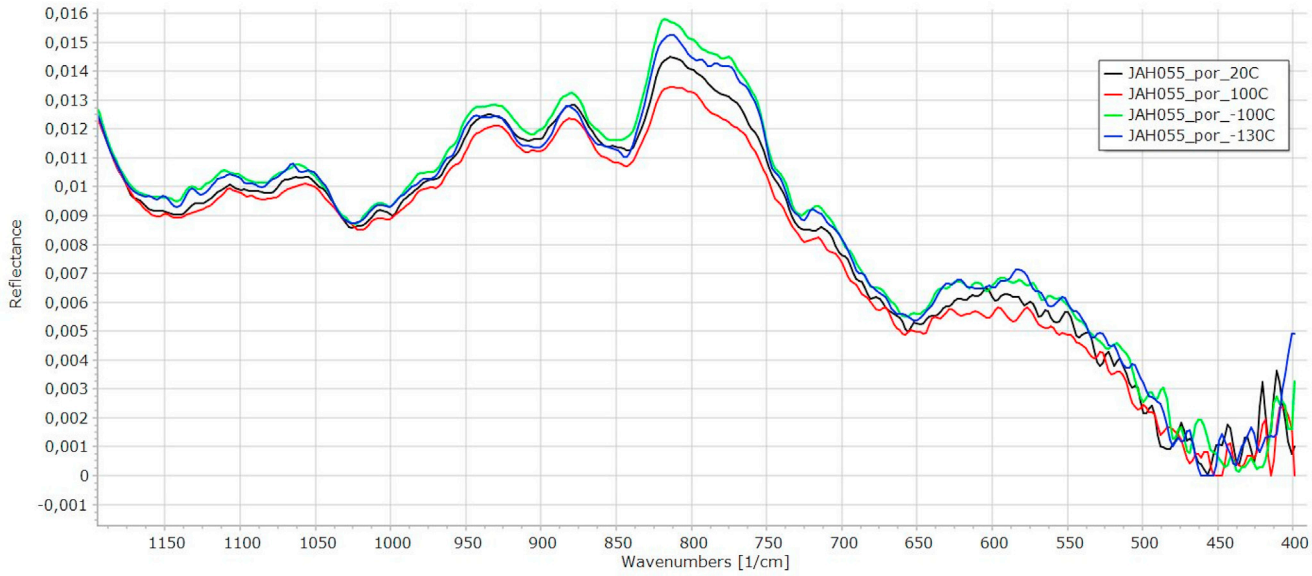

Fig. 4. Example IR reflectance curves at different temperatures for JAH 055 meteorite between +100 and −120 °C.

in the future. First the parameters of earlier instruments are presented, then the observable bands are described, and finally suggestions for their analysis are presented.

Some **instruments** have already been built or proposed for middle-infrared analysis. The MERTIS (MErcury Radiometer and Thermal Infrared Spectrometer) onboard BepiColombo (Heisinger et al., 2018) will characterize the surface radiation and reflectance of Mercury in the range of 7–14 μm (roughly 714-1428 cm^{-1}). The spectral channel width is 90 nm (0.09 μm), in the range of the laboratory spectra presented in this work (see Figs. 1 and 2), where the spectral resolution is between 90 and 200 nm for 80 spectral channels (Heisinger et al., 2010). Some experience was also gained regarding the development and testing of a somewhat simpler middle-infrared detector under the THERMAP (THERMalMApper) instrument project for the MarcoPolo-R asteroid mission proposal (Groussin et al., 2016). THERMAP would have worked between 7 and 14 μm with channel widths between 90 and 20 nm that allows studying of silicate features, including Christiansen Feature (CF), Reststrahlen Bands (RB) and Transparency Features (TF) (Hiesinger et al., 2018). The OTES (Osiris-Rex Thermal Emission Spectrometer), covering 4–50 μm range with a spectral resolution of 10 cm^{-1} (Christensen et al., 2018), looks at a single point that covers 4 m when the spacecraft is only 1 km from the asteroid. Earlier the AMICA (Asteroid Multiband Imaging Camera) detector was also installed onboard Hayabusa-1 mission, covering the range between 381 and 1008 nm in 7 bands (Ishigure et al., 2010).

The Thermal Infrared Imager (TIR) onboard Hayabusa-2 covers the 8–12 μm range with spatial resolution is 35 m at 20-km altitude and 2 m at 1-km altitude (Okada et al., 2018). The MicrOmega instrument is also part of Hayabusa 2 mission, but on the MASCOT lander (Bibring et al., 2017), and it records radiation mainly in the NIR range between 0.99 and 3.65 μm with spectral sampling of 20 cm^{-1}. The Diviner Lunar Radiometer Experiment onboard NASA's Lunar Reconnaissance Orbiter is mapping the lunar surface radiation between 0.3 and 400 μm at 9 spectral channels with on average around 250 m spatial resolution (Chin et al., 2007). A simple detector was suggested as the so-called **TIRI camera,** proposed already for the AIM and now the HERA mission that aimed to observe only around 20 bands (Foglia Manzillo et al., 2018), however the current baseline for Hera foresees a thermal infrared camera with no or very limited spectral information.

The importance of middle- and far-infrared observations was demonstrated by OTES (OSIRIS-REx Thermal Emission Spectrometer) from asteroid Bennu (Lauretta et al., 2017), covering 5.71–100 μm with accuracy of better than 3% (Christensen et al., 2018). The instrument was able to resolve 40 m from 5 km distance. For mineral identification the radiometric precision was 1/16 band depth (Ramsey and Christensen, 1998). The mission provided linked mineralogical and thermal inertia data. The measured phyllosilicate (440 cm^{-1}) and magnetite (555 and 346 cm^{-1}) features demonstrated the necessity of covering the middle- and far-infrared range (Lauretta et al., 2019b). The range of thermal inertia was found to be between 200 and 500 J m^{-2} K^{-1} $s^{-1/2}$, and global average ~350 J m^{-2} K^{-1} $s^{-1/2}$ unexpectedly, the lowest thermal inertia at the largest boulders (Rozitis et al., 2019b), but this could be spatially resolved only with high resolution thermal observations.

Based on the results on spectral characteristics discussed in this work, a spectral resolution of 0.01–0.005 μm is necessary to identify several main bands of olivine and pyroxenes, including their fine structure. **Compositional differences** related band position change for pyroxene is in the order of 0.1 μm for 10 mol% change – thus for such analysis spectral resolution in the order of 0.01 μm is necessary. The peak positions in the 10–17 μm region are good indicators of the Mg/(Mg + Fe) ratio (Koike et al., 1993), while for general characterization of silicates (identification of olivine, pyroxene, feldspar) a spectral resolution about 0.1 μm is sufficient. However for pyroxenes the changing of peak positions with Fe content is more complicated than in case of olivine.

Based on the **expected temperature range** of NEO asteroid surfaces, the differences in spectral band positions and shapes in the 100–400 K range is usually smaller than 0.1 μm. While the above listed values would require sophisticated detectors, simpler detectors could also provide useful information. It is worth considering simpler instruments, and focus on the identification of few **strong bands**. Main peaks of the main meteorite minerals using meteorite spectral data are: olivine at 11.93 μm 838 cm^{-1} (FWHM 0.09 μm = ~9.5 cm^{-1}), pyroxene at 9.77 μm 1023 cm^{-1} (FWHM ~0.01 μm = ~20 cm^{-1}), feldspar at 13.75 μm 727 cm^{-1} (FWHM ~0.002 μm = ~2.5 cm^{-1}) and 15.55 μm 645 cm^{-1} (FWHM ~22.5 cm^{-1}). As a result the analysis should focus on three main minerals in the range of about 14.0–9.09 μm (700-1100 cm^{-}) with a spectral resolution of about 0.08 μm (10 cm^{-1}), meaning roughly 30 spectral bands if they are equally distributed. The number of bands could be decreased to about the half with specifically located band positions. These parameters are more realistic for an instrument on an asteroid mission with moderate budget.

4.3. Further suggestions and future prospects

The **spatial resolution** of middle infrared data influences the spectral quality through the target grain size, as better results are expected from areas covered with smaller grains. The higher the spatial resolution of data to be gained during IR surface observation, the easier is the spectral interpretation. If the IR signal contains contribution from both, larger blocks and finer debris, it decreases the spectral quality.

The **complex consequences** of smaller grain size should be considered during the targeting of observations. Although better quality spectra is expected from finer grained powder, they could be more affected by space weathering than large blocks (Kereszturi, 2014), thus the identification of the original components or any surface fine powder might still be difficult in such areas. Based on the spacecraft observations of asteroids, smooth areas composed of fine-grained material are present and scattered over the surface. Observations should provide enough spatial resolution to be able to analyse separately the small surface units separately, and the consequence of space weathering should be also seriously considered there. Gain size also influence Thermal inertia (TI) what is lower for smaller grain size, and therefore the regolith warms up to higher temperature in daytime than for larger grain size, potentially decreasing spectral quality. The difference in the maximum daytime temperature is expected to be around 50 K in the case of Didymos, and this could produce band position shifts smaller than 0.1 μm, and a FWHM change of the same order is expected.

Based on the asteroids visited by spacecraft, finer debris covered surfaces were 50–100 m diameter on Itokawa, dust ponds on Eros were 20–60 m sized, cryovolcanic-like filled areas were around km sized on Ceres (Ruesch et al., 2016) and areas influenced by mass movements on Vesta were of km scale. Thus aiming at several tens of meters spatial resolution might provide better quality spectra for certain surfaces.

Further laboratory tests should focus on larger (mm-cm sized) grains, as they are present among the finer powder, better understanding on the consequence of mixed grain size on the reflectance spectra is required. It would also be important to develop grain size related correction formulae to modify IR reflectance curves and reflectance level in order to interpret the spectra more accurately for mineral identification. **Cosmic weathering** has an important effect on spectral shape (Jedicke et al., 2014; Kanuchova et al., 2015; Kaňuchová, Neslušan, 2007), however the analysis of irradiation on spectra of samples is not well explored especially for different grain sizes in the MIR region.

Asteroid mineralogy has so far been based mainly on visible to near-infrared spectroscopy. Certain mineral species display diagnostic near-infrared absorption features (e.g. olivine ~1 μm and pyroxene ~1 and ~2 μm Gaffey et al., 2002; de Sanctis et al., 2013), but not all of the major minerals. For example, the **silicate minerals** thought to be the main constituents of asteroid surfaces have major Si–O stretching bands in the 10 μm region. Synergic aspects are expected to emerge when comparing the **middle and near IR regions**. More detailed information is expected on **silicate components** in general by having more peaks in the MIR region. For example, plagioclases are not observable in the NIR so the MIR range might be ideal to discover and analyse them (Lim et al., 2005). Their presence could help in the reconstruction of formation condition on the moderate temperature regime (<1200 °C) both for the condensation in the solar nebula and of later alterations inside parent bodies. MIR spectral features are also useful for the identification of space weathering (e.g. Logan et al., 1973; Lucey et al., 2017; Salisbury et al., 1991).

By interpreting the observed data there are possibilities to get **further advanced and more complex results**, especially having compositional and grain size information together. The grain size analysis might provide information for the separation of seismic shaking and gas supported fluidized flow produced grain distributions (Benoit et al., 2003) by surveying the spatial distribution of different grain fractions. While mass wasting influences grains of all sizes (although the smallest ones could roll to larger distance), gas driven process hardly move larger grains and might effect only smaller ones below a certain threshold limit. Interestingly, for comets it may be different: The tensile strengths holding grains together is weaker for larger grains, and therefore they are easier to lift, as many large grains seen by Rosetta at comet 67P (Kimura et al., 2019; Reshetnyk et al., 2018). The grain size estimation for dust-pond like structures would be a unique achievement. Any potential effect of cosmic weathering might be grain size related, thus separation of the different levels of weathering signatures in spectra could be linked to characteristic grain sizes. The identification of possible impact ejected and back fallen small grains or their lack is informative on the behaviour of small grains after impact events or on their migration by exotic processes under microgravity conditions.

Summarizing, an "ideal" instrument should have spatial resolution to separate (at least) 100 m sized features on the surface from low orbit, depending on asteroid size and orbital distance. For example in the case of Didymoon (~160 m diameter) a low flyby with a close approach distance of a few times the diameter of the object produces much better spatial resolution. In general minimal spatial resolution of about 0.05° might be useful. The spectral information should be possible to connect to TI (thermal inertia) data as they support each other in the calculation of grain sizes and improve the interpretation. Detailed background datasets of laboratory spectra are also necessary for the interpretation of spectra that will be gained from a spacecraft visit to an asteroid. It is also advantageous, that the surface temperatures of main-belt asteroids are between 200 and 300 K, thus they emit thermal radiation with spectral peaks in the 10–20 μm region. Therefore their maximum thermal emission is observed in this wavelength region. As a result, MIR spectroscopy has the potential to complement the visible to near-infrared approach during asteroid analysis (Takahashi et al., 2011).

5. Conclusion

This work summarizes the possibility of investigating asteroid surfaces in the middle infrared (MIR) region by future space missions. Based on previous works and own results, meteorite spectra in the MIR (2.5–25 μm) region display more narrow, sharp, and well definable characteristic bands than in the NIR and VIS regions.

Many silicates are observable in the MIR region due to the major Si–O stretching bands there. Thus new compositional and cosmic weathering related information is accessible in the middle-IR range, including the possible identification of plagioclase on asteroid surfaces for the first time. Based on laboratory results it is possible to get estimation on the Mg/(Mg + Fe) ratio by measuring the shift of the peak positions of bands in the 10–17 μm region (Koike et al., 1993). The estimation of the Fe^{2+} content in pyroxenes might require 5 μm spectral resolution. The coupled analysis of thermal inertia and middle IR spectral shape analysis is ideal to better understand the grain size and surface processes related to the fine powder like regolith on minor bodies' unique microgravity environments.

For near-earth asteroids daytime temperatures between 200 and 300 K are expected, thus they emit most thermal radiation in the 10–20 μm region. Based on the expected temperature range, the differences in spectral band positions and shapes in the 200–400 K range are usually smaller than 0.3 μm. Both the temperature and the grain size influence the quality of spectra, with more detailed and less noisy, thus more informative spectra at lower temperatures and from smaller grains – however this does not substantially affect the peak positions (around or below the spectral resolution for most detectors). Identification of the main bands of olivine and pyroxenes using laboratory measurements of pure standards requires 0.1–0.05 μm spectral resolution, however compositional differences related to band position changes are also in this resolution range for several silicate minerals. Using moderate capability detectors, analysis of three main minerals is still possible, focusing on the range of 12.5–9.09 μm (800-1100 cm^{-1}) with spectral resolution about 0.08 μm (10 cm^{-1}), meaning roughly 30 bands if they are equally distributed. These are able to identify the expected main bands of olivine at 11.93 μm (838 cm^{-1}), pyroxene at 9.77 μm (1023 cm^{-1}), feldspar at

13.75 μm (727 cm^{-1}) and 15.5 μm (645 cm^{-1}).

Based on the existing asteroid surface observations, spatial resolution of 20–60 m might be enough to record the spectra of accumulated fine powder using >0.056° angular resolution, however for the less surveyed small (<km) asteroids smaller values might be relevant. MIR spectral observations could expand the understanding on the composition plus grain size related characteristics of dust-ponds (using linked spectral and thermal inertia data), effect of cosmic weathering and surface processes in microgravity. An ideal middle-IR instrument would provide compositional and grain size related information together. According to the argumentation presented in the paper, a thermal infrared detectors would be an important part of the payload of the planned next mission to better understand Near Earth Asteroids (Küppers et al., 2018).

Acknowledgement

This work was supported by the NEOMETLAB project of ESA regarding the meteorite access and general laboratory work (No. 4000123143/17/NL/Cbi); and the Excellence of Strategic R&D centres (GINOP-2.3.2-15-2016-00003) project of NKFIH, Hungary; and the related H2020 fund regarding meteorite and asteroids related aspects. The methodological support of Friedrich Menges for the upgrade and maintenance of Spectragryph is acknowledged, as well as the EUHUNKPT 2019 (Hungary) support. The helpful suggestions of the two referees are also welcomed.

Appendix A. Supplementary data

Supplementary data to this article can be found online at https://doi.org/10.1016/j.pss.2020.104855.

References

Adams, J.B., 1974. Visible and near-infrared diffuse reflectance spectra of pyroxenes as applied to remote sensing of solid objects in the solar system. J. Geophys. Res. 79, 4829–4831.

Adams, J.B., McCord, T.M., 1971. Alteration of lunar optical properties: age and composition effects. Science 171, 4829–4836.

Armaroli, T., Bécue, T., Gautier, S., 2004. Diffuse reflection infrared spectroscopy (DRIFTS): application to the in situ analysis of catalysts. Oil & Gas Science and Technology – Rev.IFP 59 (2), 215–237.

Barnouin, O.S., Daly, M.G., Palmer, E.E., Gaskell, R.W., Weirich, J.R., Johnson, C.L., Al Asad, M.M., Roberts, J.H., Perry, M.E., Susorney, H.C.M., Daly, R.T., Bierhaus, E.B., Seabrook, J.A., Espiritu, R.C., Nair, A.H., Nguyen, L., Neumann, G.A., Ernst, C.M., Boynton, W.V., Nolan, M.C., Adam, C.D., Moreau, M.C., Rizk, B., Drouet D'Aubigny, C.Y., Jawin, E.R., Walsh, K.J., Michel, P., Schwartz, S.R., Ballouz, R.-L., Mazarico, E.M., Scheeres, D.J., McMahon, J.W., Bottke, W.F., Sugita, S., Hirata, N., Hirata, N., Watanabe, S.-I., Burke, K.N., Dellagiustina, D.N., Bennett, C.A., Lauretta, D.S., Osiris-Rex Team, 2019. Shape of (101955) Bennu indicative of a rubble pile with internal stiffness. Nat. Geosci. 12, 247–252.

Barucci, M.A., Fornasier, S., Dotto, E., Lamy, P.L., Jorda, L., Groussin, O., Brucato, J.R., Carvano, J., Alvarez-Candal, A., Cruikshank, D., Fulchignoni, M., 2008. Asteroids 2867 Steins and 21 Lutetia: surface composition from far infrared observations with the Spitzer space telescope. Astron. Astrophys. 477, 665–670.

Beck, P., Quirico, E., Montes-Hernandez, G., Bonal, L., Bollard, J., Orthous-Daunay, F.-R., Howard, K.T., Schmitt, B., Brissaud, O., Deschamps, F., Wunder, B., Guillot, S., 2010. Hydrous mineralogy of CM and CI chondrites from infrared spectroscopy and their relationship with low albedo asteroids. Geochem. Cosmochim. Acta 74, 4881–4892.

Beck, P., Garenne, A., Quirico, E., Bonal, L., Montes-Hernandez, G., Moynier, F., Schmitt, B., 2014. Ransmission infrared spectra (2-25 μm) of carbonaceous chondrites (CI, CM, CV-CK, CR, C2 ungrouped): mineralogy, water, and asteroidal processes. Icarus 229, 263–277.

Belskaya, O.B., Danilova, I.G., Kazakov, M.O., Mironenko, R.M., Lavrenov, A.V., Likholobov, V.A., 2012. FTIR spectroscopy of adsorbed probe molecules for analyzing the surface properties of supported Pt (Pd) catalysts. In: Theophanides, T. (Ed.), Infrared Spectroscopy – Materials Science. Engineering and Technology, Croatia, p. 510.

Belton, M.J.S., Mueller, B.E.A., D'Amario, L.A., Byrnes, D.V., Klaasen, K.P., Synnott, S., Breneman, H., Johnson, T.V., Thomas, P.C., Veverka, J., Harch, A.P., Davies, M.E., Merline, W.J., Chapman, C.R., Davis, D., Denk, T., Neukum, G., Petit, J.-M., Greenberg, R., Storrs, A., Zellner, B., 1996. The discovery and orbit of 1993 (243)1 Dactyl. Icarus 120, 185–199.

Benoit, P.H., Hagedorn, N.L., Kracher, A., Sears, D.W.G., White, J., 2003. Grain size and density separation on asteroids: comparison of seismic shaking and fluidization. In: 34th Lunar and Planetary Science Conference abstract 1033.

Bibring, J.-P., Hamm, V., Langevin, Y., Pilorget, C., Arondel, A., Bouzit, M., Chaigneau, M., Crane, B., Darié, A., Evesque, C., Hansotte, J., Gardien, V., Gonnod, L., Leclech, J.-C., Meslier, L., Redon, T., Tamiatto, C., Tosti, S., Thoores, N., 2017. The MicrOmega investigation onboard Hayabusa2. Space Sci. Rev. 208, 401–412.

Binzel, R.B., DeMeo, F.E., Burt, B.J., Cloutis, E.A., Rozitis, B., Burbine, T.H., Campins, H., Clar, B.E., Emery, J.P., Hergenrotherg, C.W., Howell, E.S., Lauretta, D.S., Nolan, M.C., Mansfield, M., Pietrasz, V., Polishook, D., Scheeres, D.J., 2015. Spectral slope variations for OSIRIS-REx target Asteroid (101955) Bennu: possible evidence for a fine-grained regolith equatorial ridge. Icarus 256, 22–29.

Blichert-Toft, J., Albarède, F., 1997. The Lu-Hf isotope geochemistry of chondrites and the evolution of the mantle-crust system. Earth Planet Sci. Lett. 148, 243–258.

Burns, R.G., 1970. Mineralogical Applications to Crystal Field Theory. Cambridge Univ. Press, New York.

Burns, R.G., Huggins, F.E., 1972. Cation determinative curves for Mg–Fe–Mn olivines from vibrational spectra. Am. Mineralalogist 57, 967–985.

Bus, S.J., Binzel, R.P., Burbine, T.H., 1999. Beyond Taxonomy: Trends in the SMASS II Asteroid Data Set. American Astronomical Society. DPS meeting #31, id.11.04.

Bus, Schelte J., Binzel, Richard P., July, 2002a. Phase II of the small main-belt asteroid spectroscopic survey. A feature-based taxonomy. Icarus 158, 146–177.

Bus, S.J., Vilas, F., Barucci, M.A., 2002b. Visible-wavelength spectroscopy of asteroids. In: Bottke Jr., W.F., Cellino, A., Paolicchi, P., Binzel, R.P. (Eds.), Asteroids III. University of Arizona Press, Tucson, p. 204.

Campins, H., Emery, J.P., Kelley, M., Fernandez, Y., Licandro, J., Delbo, M., Barucci, A., Dotto, E., 2009. Spitzer observations of spacecraft target 162173 (1999 JU3). Astron. Astrophys. 503, L17–L20.

Chapman, C.R., 1994. Impacts on the Earth by asteroids and comets: assessing the hazard. Nature 367, 33–40.

Chapman, C.R., Morrison, D., Zellner, B., 1975. Surface properties of asteroids - a synthesis of polarimetry, radiometry, and spectrophotometry. Icarus 25, 104–130.

Cheng, A.F., Michel, P., Jutzi, M., Rivkin, A.S., Stickle, A., Barnouin, O., Ernst, C., Atchison, J., Pravec, P., Richardson, D.C., AIDA Team, 2016. Asteroid impact & deflection assessment mission: kinetic impactor. Planet. Space Sci. 121, 27–35.

Cheng, A., Michel, P., Rivkin, A., Barnouin, O., Stickle, A., Miller, P., Chesley, S., Richardson, D., 2017. Double asteroid redirection test (DART) element of AIDA mission. European Planetary Science Congress id EPSC2017–E2778.

Chihara, H., Koike, C., Tsuchiyama, A., Tachibana, S., Sakamoto, D., 2002. Compositional dependence of infrared absorption spectra of crystalline silicates I. Mg–Fe pyroxenes. Astron. Astrophys. 391, 267–273.

Chin, G., Brylow, S., Foote, M., Garvin, J., Kasper, J., Keller, J., Litvak, M., Mitrofanov, I., Paige, D., Raney, K., Robinson, M., Sanin, A., Smith, D., Spence, H., Spudis, P., Stern, S.A., Zuber, M., 2007. Lunar reconnaissance orbiter overview: the instrument suite and mission. Space Sci. Rev. 129, 391–419.

Christensen, P.R., Bandfield, J.L., Hamilton, V.E., Howard, D.A., Lane, M.D., Piatek, J.L., Ruff, S.W., Stefanov, W.L., 2000. A thermal emission spectral library of rock-forming minerals. J. Geophys. Res. 105 (E4), 9735–9739.

Christensen, P.R., Hamilton, V.E., Mehall, G.L., Pelham, D., O'Donnell, W., Anwar, S., Bowles, H., Chase, S., Fahlgren, J., Farkas, Z., Fisher, T., James, O., Kubik, I., Lazbin, I., Miner, M., Rassas, M., Schulze, L., Shamordola, K., Tourville, T., West, G., Woodward, R., Lauretta, D., 2018. The OSIRIS-REx thermal emission spectrometer (OTES) instrument. Space Sci. Rev. 214 (87), 39.

Clark, B.E., Hapke, B., Pieters, C., Britt, D., 2002. In: Bottke Jr., W.F., Cellino, A., Paolicchi, P., Binzel, R.P. (Eds.), Asteroid Space Weathering and Regolith Evolution. Asteroids III. University of Arizona Press, Tucson, pp. 585–599.

Cloutis, E.A., Mann, P., Izawa, M.R.M., Nathues, A., Reddy, V., Hiesinger, H., Le Corre, L., Palomba, E., 2013. The 2.5-5.1 μm reflectance spectra of HED meteorites and their constituent minerals: implications for Dawn. Icarus 225, 581–601.

Cohen, M., Witteborn, F.C., Roush, T., Bregman, J., Wooden, D., 1998. Spectral irradiance calibration in the infrared. VIII. 5-14 micron spectroscopy of the asteroids Ceres, Vesta, and pallas. Astron. J. 115 (4), 1671–1679.

Corley, L.M., Gillis-Davis, J.J., 2015. Temperature effects on the reflectance spectra of olivine and plagioclase. In: 46th Lunar and Planetary Science Conference abstract 2858.

Dahm, D.J., Dahm, K.D., 2007. Interpreting Diffuse Reflectance and Transmittance: A Theoretical Introduction to Absorption Spectroscopy of Scattering Materials. IM Publications, Chichester.

Day, K.L., 1981. Infrared extinction of amorphous iron silicates. Astrophys. J. 246, 110–112.

de León, J., Campins, H., Morate, D., De Prá, M., Alí-Lagoa, V., Licandro, J., Rizos, J.L., Pinilla-Alonso, N., DellaGiustin, D.N., Laurettag, D.S., Popescu, M., Lorenzi, V., 2018. Expected spectral characteristics of (101955) Bennu and (162173) Ryugu, targets of the OSIRIS-REx and Hayabusa2 missions. Icarus 313, 25–37.

DeMeo, F.E., Carry, B., 2013. The taxonomic distribution of asteroids from multi-filter all-sky photometric surveys. Icarus 226, 723–741.

DeMeo, F.E., Binzel, Richard P., Slivan, S.M., Bus, S.J., 2009. An extension of the Bus asteroid taxonomy into the near-infrared. Icarus 202, 160–180.

Donaldson Hanna, K.L., Thomas, I.R., Bowles, N.E., Greenhagen, B.T., Pieters, C.M., Mustard, J.F., Jackson, C.R.M., Wyatt, M.B., 2012. Laboratory emissivity measurements of the plagioclase solid solution series under varying environmental conditions. J. Geophys. Res. 117 (E11). CiteID E11004.

Donaldson Hanna, K.L., Schrader, D.L., Cloutis, E.A., Cody, G.D., King, A.J., McCoy, T.J., Applin, D.M., Mann, J.P., Bowles, N.E., Brucato, J.R., Connolly, H.C., Dotto, E., Keller, L.P., Lim, L.F., Clark, B.E., Hamilton, V.E., Lantz, C., Lauretta, D.S., Russell, S.S., Schofield, P.F., 2019. Spectral characterization of analog samples in anticipation of OSIRIS-REx's arrival at Bennu: a blind test study. Icarus 319, 701–723.

Dotto, E., Müller, T.G., Barucci, M.A., Encrenaz, Th, Knacke, R.F., Lellouch, E., Doressoundiram, A., Crovisier, J., Brucato, J.R., Colangeli, L., Mennella, V., 2000. ISO results on bright Main Belt asteroids: PHT–S observations. Astron. Astrophys. 358, 1133–1141.
Drochner, A., Vogel, G.H., 2012. Diffuse reflectance infrared fourier transform spectroscopy: an in situ method for the study of the nature and dynamics of surface intermediates. In: Schäfer, R., Schmidt, P.C. (Eds.), Methods in Physical Chemistry, first ed. Wiley, p. 846.
Duffard, R., Kumar, K., Pirrotta, S., Salatti, M., Kubínyi, M., Derz, U., Armytage, R.M.G., Arloth, S., Donati, L., Duricic, A., Flahaut, J., Hempel, S., Pollinger, A., Poulsen, S., 2011. A multiple-rendezvous, sample-return mission to two near-Earth asteroids. Adv. Space Res. 48, 120–132.
Duke, D.A., Stephens, J.D., 1964. Infrared investigation of the olivine group minerals. Am. Mineral. 49, 1388–1407.
Emery, J.P., Cruikshank, D.P., Van Cleve, J., 2006. Thermal emission spectroscopy (5.2 38 μm) of three Trojan asteroids with the Spitzer Space Telescope: detection of fine-grained silicates. Icarus 182, 496.
Emery, J.P., Rozitis, R., Christensen, P.R., Hamilton, V.E., Haberle, C., Simon, A.A., Reuter, D.C., Delbó, M., Lim, L.F., Clark, B.E., Ryan, A., Chesley, S.R., Boynton, M.V., Polit, A., Westerman, M., Becker, T., Garcia, R., Lambert, D., Kidd, J., Howell, E.S., Nolan, M.C., Enos, H.L., Lauretta, D.S., 2019. Overview of OSIRIS-REx thermal observations. In: Asteroid Science Conference abstract 2113.
Feierberg, M.A., Witteborn, F.C., Lebofsky, L.A., 1983. Detection of silicate emission features in the 8- to 13-μm spectra of main belt asteroids. Icarus 56, 393–397.
Fiege, K., Guglielmino, M., Altobelli, N., Trieloff, M., Srama, R., Orlando, T.M., 2019. Space weathering induced via microparticle impacts: 2. Dust impact simulation and meteorite target analysis. J. Geophys. Res.: Plan 124, 1084–1099.
Fintor, K., Park, C., Nagy, S., Pal-Molnar, E., Krot, A.N., 2014. Hydrothermal origin of hexagonal CaAl2Si2O8 (dmisteinbergite) in a compact Type A CAI from the Northwest Africa 2086 CV3 chondrite. Meteoritics Planet Sci. 49, 812–823.
Foglia Manzillo, F., Babić, L., Esposito, M., 2018. TIRI: a Multi-Purpose Thermal InfraRed Payload for Asteroid Observation. Didymos Observer Workshop, Prague, 2018, abstract 19.
Fraser, D.J.J., Griffith, P.R., 1990. Effect of scattering coefficient on diffuse reflectance infrared spectra and applied spectroscopy, 44, 193–199.
Fujiwara, A., Mukai, T., Kawaguchi, J., Uesugi, K.T., 2000. Sample return mission to NEA : MUSES-C. Adv. Space Res. 25, 231–238.
Fuller, M.P., Griffith, P.R., 1978. Diffuse reflectance measurements by infrared Fourier transform spectrometry. Anal. Chem. 50, 1960–1910.
Gade, R., Kaden, U., Fassler, D., 1987. Absorption spectra of molecules adsorbed on light-scattering media. Part 2.—interpretation of diffuse reflectance data. J. Chem. Soc., Faraday Trans. 2 (83), 2201–2210, 12.
Gaffey, M.J., Burbine, T.H., Binzel, R.P., 1993. Asteroid spectroscopy: progress and perspectives. Meteoritics 28, 161–187.
Gaffey, M.J., Cloutis, E.A., Kelley, M.S., Reed, K.L., 2002. Mineralogy of asteroids. In: Bottke Jr., W.F., Cellino, A., Paolicchi, P., Binzel, R.P. (Eds.), Asteroids III. University of Arizona Press, Tucson, p. 204.
Gillett, F.C., Merrill, K.M., 1975. 7.5–13.5 micron spectra of Ceres and Vesta. Icarus 26, 358–360.
Góbi, S., Kereszturi, A., Beck, P., Quirico, E., Schmidt, B., 2014. Investigating the Hydration of CM2 meteorites by IR spectroscopy. In: Conference: Workshop on the Modern Analytical Methods Applied to Earth and Planetary Sciences abstract 1821.
Green, S.F., Eaton, N., Aitken, D.K., Roche, P.F., Meadows, A.J., 1985. 8- to 13-μm spectra of asteroids. Icarus 62, 282–288.
Greenwood, R.C., Franchi, I.A., Jambon, A., Buchanan, P.C., 2005. Widespread magma oceans on asteroidal bodies in the early Solar System. Nature 435, 916–918.
Groussin, O., Licandro, J., Helbert, J., Reynaud, J.L., Levacher, P., Reyes García-Talavera, M., Alí-Lagoa, V., Blanc, P.E., Brageot, E., Davidsson, B., Delbó, M., Deleuze, M., Delsanti, A., Diaz Garcia, J.J., Dohlen, K., Ferrand, D., Green, S.F., Jorda, L., Joven Álvarez, E., Knollenberg, J., Kührt, E., Lamy, P., Lellouch, E., Le Merrer, J., Marty, B., Mas, G., Rossin, C., Rozitis, B., Sunshine, J., Vernazza, P., Vives, S., 2016. THERMAP: a mid-infrared spectro-imager for space missions to small bodies in the inner solar system. Exp. Astron. 41, 95–115.
Gundlach, B., Blum, J., 2013. A new method to determine the grain size of planetary regolith. Icarus 223, 479–492.
Gurgurewicz, J., Mège, D., Carrère, V., Kostylew, J., Purcell, P., Cornen, G., 2009. Spectrometric Characterization of Basaltic Rock Alteration in Cold and Wet (Baikalian) and Hot and Dry (Ogadenian) Conditions. European Planetary Science Congress abstract EPSC2009-176.
Hamilton, V., 2000a. Thermal infrared emission spectroscopy of the pyroxene mineral series. J. Geophys. Res. 105 (E4), 9701–9716.
Hamilton, V., 2010b. Thermal infrared (vibrational) spectroscopy of Mg–Fe olivines: a review and applications to determining the composition of planetary surfaces. Geochemistry 70, 7–33.
Hamilton, V.E., Simon, A.A., Christensen, P.R., Reuter, D.C., Clark, B.E., Barucci, M.A., Bowles, N.E., Boynton, W.V., Brucato, J.R., Cloutis, E.A., Connolly, H.C., Donaldson Hanna, K.L., Emery, J.P., Enos, H.L., Fornasier, S., Haberle, C.W., Hanna, R.D., Howell, E.S., Kaplan, H.H., Keller, L.P., Lantz, C., Li, J.-Y., Lim, L.F., McCoy, T.J., Merlin, F., Nolan, M.C., Praet, A., Rozitis, B., Sandford, S.A., Schrader, D.L., Thomas, C.A., Zou, X.-D., Lauretta, D.S., Osiris-Rex Team, 2019. Evidence for widespread hydrated minerals on asteroid (101955) Bennu. Nat. Astron. 3, 332–340.
Hamm, M., Grott, M., Kührt, E., Pelivan, I., Knollenberg, J., 2018. MASCOT radiometer MARA on board the Hayabusa2. Planet. Space Sci. 159, 1–10.
Hansen, O.L., 1976. Thermal emission spectra of 24 asteroids and the Galilean satellites. Icarus 27, 463–471.
Hapke, B., 1996. Applications of an energy transfer model to three problems in planetary regoliths: the solid-state greenhouse, thermal beaming, and emittance spectra. J. Geophys. Res. 101, 16833–16840.
Hargrove, K.D., Emery, J.P., Campins, H., Kelley, M.S.P., 2015. Asteroid (90) Antiope: another icy member of the Themis family? Icarus 254, 150–156.
Harris, A.W., 1998. A thermal model for near-earth asteroids. Icarus 131, 291–301.
Harris, A.W., Mueller, M., Lisse, C.M., Cheng, A.F., 2009. A survey of Karin cluster asteroids with the spitzer space telescope. Icarus 199, 86–96.
Hecht, H.G., 1976. The interpretation of diffuse reflectance spectra. J. Res. Nat. Bur. Stand. A. Phys. Chem. 80 (4), 567–583.
Hecht, H.G., 1980. Quantitative analysis of powder mixtures by diffuse reflectance. Appl. Spectrosc. 34, 161.
Hiesinger, H., Helbert, J., Mertis Co-I team, 2010. The Mercury radiometer and thermal infrared spectrometer (MERTIS) for the BepiColombo mission. Planet. Space Sci. 58, 144–165.
Hiesinger, H., Helbert, J., D'Amore, M., Maturilli, A., Peter, G., Walter, I., Weber, I., Bauch, K., Morlok, A., 2018. Status of the Mercury thermal radiometer and thermal infrared spectrometer (MERTIS) for BepiColombo. In: 49th Lunar and Planetary Science Conference abstract 1997.
Hinrichs, J.L., Lucey, P.G., 2002. Temperature-dependent near-infrared spectral properties of minerals, meteorites, and lunar soil. Icarus 155, 169–180.
Hinrichs, J.L., Lucey, P.G., Robinson, M.S., Meibom, A., Krot, A.N., 1999a. Implications of temperature dependent near-IR spectral properties of common minerals and meteorites for remote sensing of asteroids. Geophys. Res. Lett. 26, 1661–1664.
Hinrichs, J.L., Lucey, P.G., Robinson, M.S., Meibom, A., Krot, A.N., 1999b. Temperature dependent near-infrared spectra of olivine and H5 ordinary chondrites. In: 30th Lunar Planet Science Conference abstract 1505.
Hofmeister, A.M., Pitman, K.M., 2007. Evidence for kinks in structural and thermodynamic properties across the forsterite-fayalite binary from thin-film IR absorption spectra. Phys. Chem. Miner. 34, 319–333.
Iishi, K., Tomisaka, T., Kato, T., Umegaki, Y., 1971. Isomorphous substitution and infrared and far infrared spectra of the feldspar group. Neues Jahrbuch Mineral. Abhand. 115, 98–119.
Ishiguro, M., Nakamura, R., Tholen, D.J., Hirata, N., Demura, H., Nemoto, E., Nakamura, A.M., Higuchi, Y., Sogame, A., Yamamoto, A., Kitazato, K., Yokota, Y., Kubota, T., Hashimoto, T., Saito, J., 2010. The Hayabusa spacecraft asteroid multi-band imaging camera: AMICA. Icarus 207, 714–731.
Jäeger, C., Molster, F.J., Dorschner, J., Henning, T., Mutschke, H., Waters, L.B.F.M., 1998. Steps toward interstellar silicate mineralogy. IV. The crystalline revolution. Astron. Astrophys. 339, 904.
Jawin, E.R., Walsh, K.J., Barnouin, O.S., McCoy, T.J., Ballouz, R.-L., Molaro, J.L., Delbo, M., Pajola, M., Lauretta, D.S., Nolan, M.C., Burke, K.N., Bennett, C.A., Dellagiustina, D.N., Connolly, H.C., Daly, M.G., Scheeres, D., Susorney, H.C.M., Osiris-Rex Team, 2019. The geology of Bennu's biggest boulders. In: 50th LPSC abstract 1577.
Jedicke, R., Nesvorný, D., Whiteley, R., Ivezić, Ž., Jurić, M., 2014. An age-colour relationship for main-belt S-complex asteroids. Nature 429, 275–277.
Kanuchova, Z., Brunetto, R., Fulvio, D., Strazzulla, G., 2015. Near-ultraviolet bluing after space weathering of silicates and meteorites. Icarus 258, 289–296.
Kańuchová, Z., Neslušan, L., 2007. The parent bodies of the Quadrantid meteoroid stream. Astron. Astrophys. 470, 1123–1136.
Kereszturi, A., 2014. Surface processes in microgravity for landing and sampling site selection of asteroid missions—suggestions for MarcoPolo-R. Planet. Space Sci. 101, 65–76.
Kimura, H., Hilchenbach, M., Merouane, S., Paquette, J., Stenzel, O., 2019. The Morphological, Elastic, and Electric Properties of Dust Aggregates in Comets: A Close Look at COSIMA/Rosetta's Data on Dust in Comet 67P/Churyumov-Gerasimenko. Submitted to Planetary and Space Science.
Koike, C., Shibai, H., Tsuchiyama, A., 1993. Extinction of olivine and pyroxene in the mid- and far-infrared. Mon. Not. Roy. Astron. Soc. 264, 654–658.
Korte, E.H., 1990. Infrarot-Spectroskopie diffus reflektierender Proben. In: Gunzler, H., Borsdorf, R., Fresenius, W., Huber, W., Kelker, H., Lüderwald, I., Tiilg, G., Wisser, H. (Eds.), Analytiker Taschenbuch, 9. Springer, Berlin, pp. 9–123.
Kortum, G., 1969. Reflectance Spectroscopy: Principles, Methods, Applications. Springer, New York.
Kortum, G., Delfs, H., 1964. Reflexions spektrometrische messungen im infraroten spektral gebiet. Spectrochim. Acta 20, 405–413.
Kubelka, P., 1948. New contributions to the optics of intensely light-scattering materials. Part I. J. Opt. Soc. Am. 38, 448–457.
Kubelka, P., Munk, F., 1931. Ein Beitrag zur Optik der Farbanstriche. Zeitschrift für Technische Physik 12, 593–601.
Küppers, M., O'Rourke, L., Bockelée-Morvan, D., Zakharov, V., Lee, S., von Allmen, P., Carry, B., Teyssier, D., Marston, A., Muller, T., Crovisier, J., Barucci, M.A., Moreno, R., 2014. Localized sources of water vapour on the dwarf planet (1)Ceres. Nature 505, 525.
Küppers, M., Cheng, A., Carnelli, I., 2018. The Hera mission: European component of the asteroid impact and deflection assessment (AIDA) mission to a binary asteroid. In: 49th Lunar and Planetary Science Conference abstract 1144.
Lamy, P.L., Groussin, O., Fornasier, S., Jorda, L., Kaasalainen, M., Barucci, M.A., 2010. Thermal properties of asteroid 21 Lutetia from spitzer space telescope observations. Astron. Astrophys. 516, A74.
Landsman, Z.A., Licandrob, J., Campins, H., Zifferd, J., dePrá, M., Cruikshank, D.P., 2016. The veritas and Themis asteroid families: 5–14 μm spectra with the spitzer space telescope. Icarus 269, 62–74.

Landsman, Z.A., Emery, J.P., Campins, H., Hanuš, J., Lim, L.F., Cruikshank, D.P., 2018. Asteroid (16) Psyche: evidence for a silicate regolith from spitzer space telescope spectroscopy. Icarus 304, 58–73.
Lane, M.D., 2011. Midinfrared spectroscopy of synthetic olivines: thermal emission, specular and diffuse reflectance, and attenuated total reflectance studies of forsterite to fayalite. J. Geophys. Res. 116, E08010.
Lantz, C., Brunetto, R., Barucci, M.A., Dartois, E., Duprat, J., Engrand, C., Godard, M., Ledu, D., Quirico, E., 2015. Ion irradiation of the Murchison meteorite: visible to mid-infrared spectroscopic results. Astron. Astrophys. 577 (A41), 9.
Lantz, C., Brunetto, R., Barucci, M.A., Fornasier, S., Baklouti, D., Bourçois, J., Godard, M., 2017. Ion irradiation of carbonaceous chondrites: a new view of space weathering on primitive asteroids. Icarus 285, 43–57.
Lantz, C., Binzel, R.P., DeMeo, F.E., 2018. Space weathering trends on carbonaceous asteroids: a possible explanation for Bennu's blue slope? Icarus 302, 10–17.
Lauretta, D.S., Balram-Knutson, S.S., Beshore, E., Boynton, W.V., Drouet d'Aubigny, C., DellaGiustina, D.N., Enos, H.L., Golish, D.R., Hergenrother, C.W., Howell, E.S., Bennett, C.A., Morton, E.T., Nolan, M.C., Rizk, B., Roper, H.L., Bartels, A.E., Bos, B.J., Dworkin, J.P., Highsmith, D.E., Lorenz, D.A., Lim, L.F., Mink, R., Moreau, M.C., Nuth, J.A., Reuter, D.C., Simon, A.A., Bierhaus, E.B., Bryan, B.H., Ballouz, R., Barnouin, O.S., Binzel, R.P., Bottke, W.F., Hamilton, V.E., Walsh, K.J., Chesley, S.R., Christensen, P.R., Clark, B.E., Connolly, H.C., Crombie, M.K., Daly, M.G., Emery, J.P., McCoy, T.J., McMahon, J.W., Scheeres, D.J., Messenger, S., Nakamura-Messenger, K., Righter, K., Sandford, S.A., 2017. OSIRIS-REx: sample return from asteroid (101955) Bennu. Space Sci. Rev. 212, 925–984.
Lauretta, D.S., Dellagiustina, D.N., Bennett, C.A., Golish, D.R., Becker, K.J., Balram-Knutson, S.S., Barnouin, O.S., Becker, T.L., Bottke, W.F., Boynton, W.V., Campins, H., Clark, B.E., Connolly, H.C., Drouet D'Aubigny, C.Y., Dworkin, J.P., Emery, J.P., Enos, H.L., Hamilton, V.E., Hergenrother, C.W., Howell, E.S., Izawa, M.R.M., Kaplan, H.H., Nolan, M.C., Rizk, B., Roper, H.L., Scheeres, D.J., Smith, P.H., Walsh, K.J., Wolner, C.W.V., Osiris-Rex Team, 2019. The unexpected surface of asteroid (101955) Bennu. Nature 568, 55–60.
Lauretta, D.S., Al Asad, M.M., Ballouz, R.-L., Barnouin, O.S., Bierhaus, E.B., Boynton, W.V., Breitenfeld, L.B., Calaway, M.J., Chojnacki, M., Christensen, P.R., Clark, B.E., Connolly, H.C., Drouet, d'Aubigny C., Daly, M.G., Daly, R.T., Delbó, M., DellaGiustina, D.N., Dworkin, J.P., Emery, J.P., Enos, H.L., Farnocchia, D., Golish, D.R., Haberle, C.W., Hamilton, V.E., Hergenrother, C.W., Jawin, E.R., Kaplan, H.H., Le Corre, L., McCoy, T.J., McMahon, J.W., Michel, P., Molaro, J.L., Nolan, M.C., Pajola, M., Palmer, E., Perry, M.E., Reuter, D.C., Rizk, B., Roberts, J.H., Ryan, A., Scheeres, D.J., Schwartz, S.R., Simon, A.A., Susorney, H.C.M., Walsh, K.J., Zou, X.-D., the OSIRIS-REx Team, 2019a. OSIRIS-REx arrives at asteroid (101955) Bennu: exploration of a hydrated primitive Near-Earth Asteroid. In: 50th Lunar and Planetary Science Conference abstract 2608.
Lazzaro, D., Angeli, C.A., Carvano, J.M., Mothé-Diniz, T., Duffard, R., Florczak, M., 2004. S3OS2: the visible spectroscopic survey of 820 asteroids. Icarus 172, 179–220.
Le Bras, A., Erard, S., 2003. Reflectance spectra of regolith analogs in the midinfrared: effects of grain size. Planet. Space Sci. 51, 281–294.
Licandro, J., Campins, H., Kelley, M., Hargrove, K., Pinilla-Alonso, N., Cruikshank, D., Rivkin, A.S., Emery, J., 2011. Cybele: detection of small silicate grains, water-ice, and organics. Astron. Astrophys. 525, A34, 65.
Lim, L.F., McConnochie, T.H., Bell III, J.F., Hayward, T.L., 2005. Thermal infrared (8–13 μm) spectra of 29 asteroids: the cornell mid-infrared asteroid spectroscopy (MIDAS) survey. Icarus 173, 385–408.
Lim, L.F., Emery, J.P., Moskovitz, N.A., 2011. Mineralogy and thermal properties of V-type Asteroid 956 Elisa: evidence for diogenitic material from the Spitzer IRS (5-35 μm) spectrum. Icarus 213, 510–523.
Lisse, C.M., VanCleve, J., Adams, A.C., A'Hearn, M.F., Fernandez, Y.R., Farnham, T.L., Armus, L., Grillmair, C.J., Ingalls, J., Belton, M.J.S., Groussin, O., McFadden, L.A., Meech, K.J., Schultz, P.H., Clark, B.C., Feaga, L.M., Sunshine, J.M., 2006. Spitzer spectral observations of the Deep impact ejecta. Science 313, 635.
Logan, L.M., Hunt, G.R., Salisbury, J.W., Balsamo, S.R., 1973. Compositional implications of Christiansen frequency maximums for infrared remote sensing applications. J. Geophys. Res. 78, 4983.
Losiak, A., Jõeleht, A., Plado, J., Szyszka, M., Wild, E.M., Bronikowska, M., Belcher, C., Kirsimäe, K., Steier, P., 2017. Formation (and dating) of small impact craters on Earth as an analogue for Mars (Ilumetsa Craters Estonia). In: 19th EGU General Assembly, p. 17147.
Lucey, P.G., Greenhagen, B.T., Song, E., Arnold, J.A., Lemelin, M., Hanna, K.D., Bowles, N.E., Glotch, T.D., Paige, D.E., 2017. Space weathering effects in Diviner Lunar Radiometer multispectral infrared measurements of the lunar Christiansen Feature: characteristics and mitigation. Icarus 283, 343–351.
MacPherson, G.J., Davis, A.M., Zinner, E.K., 1995. The distribution of aluminum-26 in the early Solar System - a reappraisal. Meteoritics 30, 365.
Mainzer, A., Usui, F., Trilling, D.E., 2015. In: Bottke, William F. (Ed.), Space-Based Thermal Infrared Studies of Asteroids. Asteroids IV, Patrick Michel, Francesca E. DeMeo. University of Arizona Press, Tucson, ISBN 978-0-816-53213-1, p. 895, 89-106.
Mandelis, A., Boroumand, F., Van den Bergh, H., 1991. Quantitative diffuse reflectance and transmittance spectroscopy of loosely packed powders. Spectrochim. Acta, Part A 47 (7), 943–971.
Mason, B., 1968. Pyroxenes in meteorites. Lithos 1, 1–11.
Matsumoto, T., Hasegawa, S., Nakao, S., Sakai, M., Yurimoto, H., 2017. Population characteristics of submicrometer-sized craters on regolith particles from asteroid Itokawa. Icarus 303, 22–33.
Maturilli, A., Helbert, J., Witzke, A., Moroz, L., 2006. Emissivity measurements of analogue materials for the interpretation of data from PFS on Mars Express and MERTIS on Bepi-Colombo. Planet. Space Sci. 54, 1057–1064.
McAdam, M.M., Sunshine, J.M., Howard, K.T., McCoy, T.M., 2015. Aqueous alteration on asteroids: linking the mineralogy and spectroscopy of CM and CI chondrites. Icarus 245, 320–332.
Melamed, N.T., 1963. Optical properties of powders. Part I. Optical absorption coefficients and the absolute value of the diffuse reflectance. Part II. Properties of luminescent powders. J. Appl. Phys. 34, 560–570.
Michel, P., Barucci, M.A., Cheng, A.F., Böhnhardt, H., Brucato, J.R., Dotto, E., Ehrenfreund, P., Franchi, I.A., Green, S.F., Lara, L.-M., Marty, B., Koschny, D., Agnolon, D., 2014. MarcoPolo-R: near-Earth Asteroid sample return mission selected for the assessment study phase of the ESA program cosmic vision. Acta Astronaut. 93, 530–538.
Michel, Patrick, Cheng, A., Küppers, M., Pravec, P., Blum, J., Delbo, M., Green, S.F., Rosenblatt, P., Tsiganis, K., Vincent, J.B., Biele, J., Ciarletti, V., Hérique, A., Ulamec, S., Carnelli, I., Galvez, A., Benner, L., Naidu, S.P., Barnouin, O.S., Richardson, D.C., Rivkin, A., Scheirich, P., Moskovitz, N., Thirouin, A., Schwartz, S.R., Campo Bagatin, A., Yu, Y., 2016. Science case for the asteroid impact mission (AIM): a component of the asteroid impact & deflection assessment (AIDA) mission. Adv. Space Res. 57, 2529–2547.
Michel, P., Kueppers, M., Sierks, H., Carnelli, I., Cheng, A.F., Mellab, K., Granvik, M., Kestilä, A., Kohout, T., Muinonen, K., et al., 2018. European Component of the AIDA Mission to a Binary Asteroid: Characterization and Interpretation of the Impact of the DART Mission, vol. 62. Advances in Space Research, Elsevier, pp. 2261–2272, 8.
Michikami, T., Honda, C., Miyamoto, H., Hirabayashi, M., Hagermann, A., Irie, T., Nomura, K., Ernst, C.M., Kawamura, M., Sugimoto, K., Tatsumi, E., Morota, T., Hirata, N., Noguchi, T., Cho, Y., Kameda, S., Kouyama, T., Yokota, Y., Noguchi, R., Hayakawa, M., Hirata, N., Honda, R., Matsuoka, M., Sakatani, N., Suzuki, H., Yamada, M., Yoshioka, K., Sawada, H., Hemmi, R., Kikuchi, H., Ogawa, K., Watanabe, S., Tanaka, S., Yoshikawa, M., Tsuda, Y., Sugita, S., 2019. Boulder size and shape distributions on asteroid Ryugu. Icarus 331, 179–191.
Mitchell, M.B., 1993. Fundamentals and applications of diffuse reflectance infrared fourier transform (DRIFT) spectroscopy. In: Urban, M.W., Craver, C.D. (Eds.), Structure-Property Relations in Polymers, Advances in Chemistry Series, vol. 236. American Chemical Society, pp. 351–371.
Morlok, A., Koike, C., Tomioka, N., Mann, I., Tomeoka, K., 2010. Mid-infrared spectra of the shocked Murchison CM chondrite: comparisonwith astronomical observations of dust in debris disks. Icarus 207, 45–53.
Moroz, L., Schade, U., Wäsch, R., 2000. Reflectance spectra of olivine orthopyroxene-bearing assemblages at decreased temperatures: implications for remote sensing of asteroids. Icarus 147, 79–93.
Mueller, M., Marchis, F., Emery, J.P., Harris, A.W., Mottola, S., Hestroffer, D., Berthier, J., di Martino, M., 2010. Eclipsing binary trojan asteroid Patroclus: thermal inertia from spitzer observations. Icarus 205, 505–515.
Munoz Caro, G.M., Martinez-Frias, J., 2007. In: Krueger, H., Graps, A. (Eds.), Carbonaceous Dust in Planetary Systems: Origin and Astrobiological Significance. Workshop on Dust in Planetary Systems (ESA SP-643), pp. 133–138.
Nakamura, T., Noguchi, T., Tanaka, M., Zolensky, M.E., Kimura, M., Tsuchiyama, A., Nakato, A., Ogami, T., Ishida, H., Uesugi, M., Yada, T., Shirai, K., Fujimura, A., Okazaki, R., Sandford, S., Wakita, S., Ishibashi, Y., Abe, M., Okada, T., Ueno, M., Mukai, T., Yoshikawa, M., Kawaguchi, J., 2011. Itokawa dust particles: a direct link between S-type asteroids and ordinary chondrites. Science 333, 1113–1116.
Nakamura, E., Makishima, A., Moriguti, T., Kobayashi, K., Tanaka, R., Kunihiro, T., Tsujimori, T., Sakaguchi, C., Kitagawa, H., Ota, T., Yachi, Y., Yada, T., Abe, M., Fujimura, A., Ueno, M., Mukai, T., Yoshikawa, M., Kawaguchi, J., 2012. Space environment of an asteroid preserved on micrograins returned by the Hayabusa spacecraft. Proc. Natl. Acad. Sci. Unit. States Am. 109 (11), E624–E629.
Nakamura, T., Matsuoka, M., Amano, K., Kobayashi, S., Mita, H., Brunetto, R., Lantz, C., Hiroi, T., Zolensky, M.E., Kitazato, K., Sugita, S., Honda, R., Morota, T., Tatsumi, E., Milliken, R.E., Iwata, T., Kameda, S., Sawada, H., Abe, M., Ohtake, M., Matsuura, S., Arai, T., Nakauchi, Y., Mogi, K., Yamashita, S., Sato, Y., Ka, H., Honda, C., Yokota, Y., Yamada, M., Kouyama, T., Sakatani, N., Senshu, H., Hirata, N., Suzuki, H., Yoshioka, K., Hayakawa, M., Cho, Y., Pilorget, C., Poulet, F., Riu, L., Bibring, J.P., Takir, D., Domingue, D.L., Vilas, F., Barucci, M.A., Perna, D., Palomba, E., Galiano, A., Tsumura, K., Osawa, T., Komatsu, M., Nakato, A., Arai, T., Takato, N., Matsunaga, T., Imae, N., Yamaguchi, A., Kojima, H., Nakazawa, S., Tanaka, S., Yoshikawa, M., Watanabe, S., Tsuda, Y., 2019. Possible interpretations of visible/near-infrared spectra of asteroid Ryugu obtained by the Hayabusa-2 mission. In: 50th Lunar and Planetary Science Conference abstract 1681.
Nash, D.B., Salisbury, J.W., 1991. Infrared reflectance spectra (2.2–15 μm) of plagioclase feldspars. Geophys. Res. Lett. 18, 1151–1154.
Nesvorný, D., Vokrouhlický, D., Morbidelli, A., Bottke, W.F., 2009. Asteroidal source of L chondrite meteorites. Icarus 200, 698–701.
Noguchi, T., Nakamura, T., Kimura, M., Zolensky, M.E., Tanaka, M., Hashimoto, T., Konno, M., Nakato, A., Ogami, T., Fujimura, A., Abe, M., Yada, T., Mukai, T., Ueno, M., Okada, T., Shirai, K., Ishibashi, Y., Okazaki, R., 2011. Incipient space weathering observed on the surface of Itokawa dust particles. Science 333, 1121.
Okada, T., Fukuhara, T., Tanaka, S., Taguchi, M., Arai, T., Senshu, H., Sakatani, N., Ogawa, Y., Demura, H., Kitazato, K., Kouyama, T., Sekiguchi, T., Hasegawa, S., Matsunaga, T., Wada, T., Imamura, T., Takita, J., Shimaki, Y., Kyoda, H., Aoki, Y., Helbert, J., Mueller, T.G., Hagermann, A., 2018. Thermal infrared imager TIR on Hayabusa2 and its preparation for asteroid proximity phase operations around 162173 Ryugu. In: 49th LPSC abstract 1403.
Okada, T., Fukuhara, T., Tanaka, S., Taguchi, M., Arai, T., Sakatani, N., Shimaki, Y., Senshu, H., Ogawa, Y., Demura, H., Suko, K., Kitazato, K., Kouyama, T., Sekiguchi, T., Takita, J., Hasegawa, S., Matsunaga, T., Wada, T., Imamura, T., Helbert, J., Mueller, T.G., Hagermann, A., Biele, J., Grott, M., Hamm, M., Delbo, M., Yamamoto, Y., Hirata, N., Hirata, N., Terui, F., Saiki, T., Nakazawa, S.,

Yoshikawa, M., Watanabe, S., Tsuda, Y., Hayabusa2 Thermal-Infrared Imager (TIR) Team, 2019. Thermal imaging of c-type near earth asteroid 162173 Ryugu by thermal infrared imager TIR on Hayabusa2. In: 50th Lunar and Planetary Science Conference abstract 1325.

Perna, D., Barucci, M.A., Fulchignoni, M., 2013. The near-Earth objects and their potential threat to our planet. Astron. AstroPhys. Rev. 21 article id.65.

Przylibski, T.A., Zagożdżon, P.P., Kryza, R., Pilski, A.S., 2005. The Zakłodzie enstatite meteorite: mineralogy, petrology, origin, and classification. Meteoritics Planet Sci. 40, 185–200.

Ramsey, M.S., Christensen, P.R., 1998. Mineral abundance determination: quantitative deconvolution of thermal emission spectra. J. Geophys. Res. 103, 577–596.

Reddy, V., Dunn, T.L., Thomas, C.A., Moskovitz, N.A., Burbine, T.H., 2015. Mineralogy and surface composition of asteroids. In: Michel, P., et al. (Eds.), Asteroids IV. Univ. of Arizona, Tucson, pp. 43–63.

Reichenbächer, M., Popp, J., 2012. Challenges in Molecular Structure Determination. Springer, p. 437.

Reshetnyk, V.M., Skorov, Yu V., Lacerda, P., Hartogh, P., Rezac, L., 2018. Dynamics of dust particles of different structure: application to the modeling of dust motion in the vicinity of the nucleus of comet 67P/Churyumov-Gerasimenko. Sol. Syst. Res. 52, 266–281.

Reynard, B., 1991. Single-crystal infrared reflectivity of pure Mg2SiO4 forsterite and $(Mg_{0.86}, Fe_{0.14})_2SiO_4$ olivine. New data and a reappraisal. Phys. Chem. Miner. 18, 19–25.

Riu, R., Kitazato, K., Milliken, R., Iwata, T., Abe, M., Ohtake, M., Matsuura, S., Arai, T., Nakauchi, Y., Nakamura, T., Mastuoka, M., Senshu, H., Hirata, N., Hiroi, T., Pilorget, C., Brunetto, R., Poulet, F., Bibring, J.P., Takir, D., Domingue, D.L., Vilas, F., Barucci, M.A., Perna, D., Palomba, E., Galiano, A., Tsumura, K., Osawa, T., Lomatsu, M., Nakato, A., Arai, T., Takato, N., Matsunaga, T., Takagi, Y., Matsumoto, K., Kouyama, T., Yokota1, Y., Tatsumi, E., Sakatani, N., Yamamoto, Y., Okada, T., Sugita, S., Honda, R., Motora, T., Kameda, S., Sawada, H., Honda, C., Yamada, M., Suzuki, H., Yoshioka, K., Hayakawa, M., Owaga, K., Cho, Y., Takei, V., Saiki, T., Nakazawa, S., Tanaka, S., Yoshikawa, M., Watanabe, S., Tsuda, Y., 2019. Global View of the Mineralogy and Surface Properties of the Asteroid Ryugu Using NIRS3 Near-Infrared Spectrometer on Board Hayabusa-2. 50th Lunar and Planetary Science Conference abstract 1154.

Rizk, B., DellaGiustina, D.N., Golish, D.R., Bennett, C.A., Drouet, d'Aubigny C., Becker, K.J., Smith, P.H., Le Corre, L., Burke, K.N., Hergenrother, C., Ballouz, R., Clark, B.E., Nolan, M.C., Enos, E.N., Lauretta, D.S., the OSIRIS-REx Team, 2019. Results from early resolved images of asteroid Bennu. In: 50th Lunar and Planetary Science Conference abstract 1717.

Robinson, M.S., Thomas, P.C., Veverka, J., Murchie, S.L., Wilcox, B.B., 2002. The geology of 433 Eros. Meteoritics Planet Sci. 37, 1651–1684.

Roush, T.L., 1984. Effects of Temperature on Remotely Sensed Mafic Mineral Absorption Features. Masters thesis. University of Hawaii.

Roush, T.L., Singer, R.B., 1986. Gaussian analysis of temperature effects on the reflectance spectra of mafic minerals in the 1-um region. J. Geophys. Res. 91 (B10), 10301–10308.

Rozitis, B., Emery, J.O., Ryan, A., Christensen, P.R., Hamilton, V.E., Simon, A.A., Reuter, D.C., Clark, B.E., Delbo, M., Howell, E.S., Lim, L.F., Nolan, M.C., Susorney, H.C.M., Walsh, K.J., Lauretta, D., the OSIRIS-REx Team, 2019a. Thermal Inertia and Surface Roughness Maps of (101955) Bennu from OSIRIS-REx Infrared Observations. Asteroid Science abstract 2055.

Rozitis, B., Emery, J.O., Ryan, A., Christensen, P.R., Hamilton, V.E., Simon, A.A., Reuter, D.C., Clark, B.E., Delbo, M., Howell, E.S., Lim, L.F., Nolan, M.C., Susorney, H.C.M., Walsh, K.J., Lauretta, D., the OSIRIS-REx Team, 2019b. Thermal inertia maps of (101955) Bennu from OSIRIS-REx infrared observations. EPSC Abstracts 13. EPSC-DPS2019-548-1.

Ruesch, O., Platz, T., Schenk, P., McFadden, L.A., Castillo-Rogez, J.C., Quick, L.C., Byrne, S., Preusker, F., O'Brien, D.P., Schmedemann, N., Williams, D.A., Li, J.Y., Bland, M.T., Hiesinger, H., Kneissl, T., Neesemann, A., Schaefer, M., Pasckert, J.H., Schmidt, B.E., Buczkowski, D.L., Sykes, M.V., Nathues, A., Roatsch, T., Hoffmann, M., Raymond, C.A., Russell, C.T., 2016. Cryovolcanism on Ceres. Science 353 (6303) aaf4286.

Salisbury, J.W., Walter, L.S., 1989. Thermal infrared (2.5-13.5 μm) spectroscopic remote sensing of igneous rock types on a particulate planetary surfaces. J. Geophys. Res. 94, 9192–9202.

Salisbury, J.W., Hapke, B., Eastes, J.W., 1987. Usefulness of weak bands in midinfrared remote sensing of particulate planetary surfaces. J. Geophys. Res. 92, 702–710.

Salisbury, J.W., D'Aria, D.M., Jarosewich, E., 1991. Midinfrared (2.5-13.5 μm) reflectance spectra of powdered stony meteorites. Icarus 92, 280–297.

Schade, U., Wäsch, R., 1999. NIR reflectance spectroscopy of mafic minerals in the temperature region between 80 and 473 K. Adv. Space Res. 23, 1253–1256.

Simmons, E.L., 1975. Diffuse reflectance spectroscopy: a comparison of the theories. Appl. Optic. 14 (6), 1380–1386.

Singer, R.B., Roush, T.L., 1985. Effects of temperature on remotely sensed mineral absorption features. J. Geophys. Res. 90 (B14), 12434–12444.

Smith, B.C., 2011. Fundamentals of fourier transform infrared spectroscopy. Appl. Spectrosc. 139. ISBN 978142006929, CRC Press.

Stickle, A., Cheng, A.F., Michel, P., Barnouin, O.S., Campo, B.A., Miller, P.L., Pravec, P., Richardson, D.C., Schwartz, S.R., Tsiganis, K., Ulamec, S., AIDA Impact Modeling and Simulation Working Group, 2016. The Double Asteroid Redirection Test (DART) for the AIDA Mission. American Astronomical Society. DPS meeting #48, id.123.21.

Sugimoto, C., Tatsumi, E., Sugita, S., Riu, L., Nakamura, T., Morota, T., Matsuoka, M., Kitazato, K., 2019. Bright Spots on Ryugu Observed by ONC-T. Asteroid Science abstract 2051.

Sullivan, R., Greeley, R., Pappalardo, R., Asphaug, E., Moore, J.M., Morrison, D., Belton, M.J.S., Carr, M., Chapman, C.R., Geissler, P., Greenberg, R., Granahan, J., Head III, J.W., Kirk, R., McEwen, A., Lee, P., Thomas, P.C., Veverka, J., 1996. Geology of 243 Ida. Icarus 120, 119–139.

Sunshine, J.M., Bus, S.J., Corrigan, C.M., McCoy, T.J., Burbine, T.H., 2007. Olivine-dominated asteroids and meteorites: distinguishing nebular and igneous histories. Meteoritics Planet Sci. 42, 155–170.

Takahashi, J., Itoh, Y., Takahashi, S., 2011. Mid-infrared spectroscopy of 11 main-belt asteroids. Publ. Astron. Soc. Jpn. 63, 499–511.

Tholen, D.J., 1984. Asteroid Taxonomy from Cluster Analysis of Photometry. University of Arizona, Tucson.

Thompson, M.M., Palmer, R.A., 1988. In situ Fourier transform infrared diffuse reflectance and photoacoustic spectroscopy characterization of sulfur-oxygen species resulting from the reaction of SO_2 with $CaCO_3$. Appl. Spectrosc. 42, 945–951.

Vernazza, P., Carry, B., Emery, J., Hora, J.L., Cruikshank, D., Binzel, R.P., Jackson, J., Helbert, J., Maturilli, A., 2010. Mid-infrared spectral variability for compositionally similar asteroids: implications for asteroid particle size distributions. Icarus 207, 800–809.

Vernazza, P., Delbo, M., King, P.L., Izawa, M.R.M., Olofsson, J., Lamy, P., Cipriani, F., Binzel, R.P., Marchis, F., Merín, B., Tamanai, A., 2012. High surface porosity as the origin of emissivity features in asteroid spectra. Icarus 221, 1162–1172.

Vernazza, P., Fulvio, D., Brunetto, R., Emery, J.P., Dukes, C.A., Cipriani, F., Witasse, O., Schaible, M.J., Zanda, B., Strazzula, G., Baragiola, R.A., 2013. Paucity of Tagish Lake-like parent bodies in the asteroid belt and among Jupiter Trojans. Icarus 225, 517–525.

Veverka, J., Helfenstein, P., Lee, P., Thomas, P., McEwen, A., Belton, M., Klaasen, K., Johnson, T.V., Granahan, J., Fanale, F., Geissler, P., Head III, J.W., 1996. Ida and Dactyl: spectral reflectance and color variations. Icarus 120, 66–76.

Wang, Z., Zeng, X., Barlage, M., Dickinson, R.E., Gao, F., Schaaf, C.B., 2004. Using MODIS BRDF and albedo data to evaluate global model land surface albedo. J. Hydrometeorol. 5, 3–14.

Wendlandt, W.W., Hecht, J.G., 1966. Reflectance Spectroscopy. Interscience, New York, 1966.

Yano, H., Kubota, T., Miyamoto, H., Okada, T., Scheeres, D., Takagi, Y., Yoshida, K., Abe, M., Abe, S., Barnouin-Jha, O., Fujiwara, A., Hasegawa, S., Hashimoto, T., Ishiguro, M., Kato, M., Kawaguchi, J., Mukai, T., Saito, J., Sasaki, S., Yoshikawa, M., 2006. Touchdown of the Hayabusa spacecraft at the muses sea on Itokawa. Science 312, 1350–1353.

Yu, L., Ji, J., 2015. Thermophysical characteristics of OSIRIS-REx target asteroid (101955) Bennu. MNRAS 452, 368–375, 2015.